*DOI:*
10.1158/1078-0432.CCR-19-3827

*Document Version*
Peer reviewed version

**T cell dynamics in chronic lymphocytic leukemia under different treatment modalities**

Anna Vardi[1,2,3], Elisavet Vlachonikola[1,4], Despoina Papazoglou[5], Fotis Psomopoulos[1,3], Kostantia Kotta[1], Nikolaos Ioannou[5], Chrysi Galigalidou[1,6], Katerina Gemenetzi[1,6], Kostantinos Pasentsis[1], Maria Kotouza[1], Evdoxia Koravou[2], Lydia Scarfó[7], Michail Iskas[2], Niki Stavroyianni[2], Paolo Ghia[7], Achilles Anagnostopoulos[2], Anastasia Kouvatsi[4], Alan G Ramsay[5], Kostas Stamatopoulos[1,3], Anastasia Chatzidimitriou[1,3]

[1]Institute of Applied Biosciences, CERTH, Thessaloniki, Greece; [2]Hematology Department and HCT Unit, G. Papanicolaou Hospital, Thessaloniki, Greece; [3]Department of Molecular Medicine and Surgery, Karolinska Institutet, Stockholm, Sweden; [4]Faculty of Sciences, Department of Genetics, Development and Molecular Biology, Aristotle University of Thessaloniki, Thessaloniki, Greece; [5]Lymphoma Immunology Group, School of Cancer and Pharmaceutical Sciences, Faculty of Life Sciences & Medicine, King's College London, London, United Kingdom; [6]Democritus University of Thrace, Department of Molecular Biology and Genetics, Alexandroupolis, Greece; [7]Division of Experimental Oncology, Università Vita-Salute San Raffaele and IRCCS Ospedale San Raffaele, Milan, Italy

**SHORT TITLE**: CLL T cell immunoprofiling over treatment

**CONFLICT-OF-INTEREST DISCLOSURE**

KS and AC received research funding from Janssen.

**CORRESPONDING AUTHOR:**

Anastasia Chatzidimitriou, PhD

Institute of Applied Biosciences, CERTH

57001 Thessaloniki, GREECE

Phone: +30.2310.498271

Fax: +30.2310.498270

e-mail: achatzidimitriou@certh.gr

Text word count: 4601

Abstract word count: 244

Number of figures: 6

Number of references: 45

Number of supplemental files: 1

**TRANSLATIONAL RELEVANCE**

Chronic lymphocytic leukemia (CLL) T cells display largely defective anti-tumor responses. From a clinical perspective, there is a clear need to optimize CLL immunotherapy, especially regarding minimal residual disease eradication. Boosting anti-tumor T cell responses could ideally fit this gap, and identifying the best combination treatment partners is of translational relevance.

We investigated the effect of treatment on CLL T cells in relation to: (i) treatment type (FCR versus ibrutinib versus rituximab-idelalisib), and (ii) clinical response.

In contrast to chemoimmunotherapy, B-cell receptor signaling inhibitors (BcRi) preserved pre-treatment T cell clones, which expanded further as treatment continued and the clinical response deepened. We found major clonotypes shared among different patients, raising the possibility of selection by conserved, CLL-associated epitopes. A concurrent restoration of T cell functionality with BcRi therapy arguably contributed to clinical response. Overall, this data provides rationale for designing combination strategies aiming to boost cytotoxic anti-tumor responses.

**ABSTRACT**

**Background:** Using next-generation sequencing (NGS), we recently documented T cell oligoclonality in treatment-naive chronic lymphocytic leukemia (CLL), with evidence indicating T cell selection by restricted antigens.

**Experimental Design:** Here, we sought to comprehensively assess T cell repertoire changes during treatment in relation to: (i) treatment type [fludarabine-cyclophosphamide-rituximab (FCR) versus ibrutinib (IB) versus rituximab-idelalisib (R-ID)], and (ii) clinical response, by combining NGS immunoprofiling, flow cytometry and functional bioassays.

**Results:** T cell clonality significantly increased at: (i) 3 months in the FCR and R-ID treatment groups, and (ii) over deepening clinical response in the R-ID group, with a similar trend detected in the IB group. Notably, in constrast to FCR that induced T cell repertoire reconstitution, B cell receptor signaling inhibitors (BcRi) preserved pre-treatment clones. Extensive comparisons both within CLL as well as against T cell receptor sequence databases showed little similarity with other entities, but instead revealed major clonotypes shared exclusively by CLL patients, alluding to selection by conserved CLL-associated antigens. We then evaluated the functional effect of treatments on T cells and found that: (i) R-ID upregulated the expression of activation markers in effector memory T cells, and (ii) both BcRi improved anti-tumor T cell immune synapse formation, in marked contrast to FCR.

**Conclusions:** Taken together, our NGS immunoprofiling data suggest that BcRi retain T cell clones that may have developed against CLL-associated antigens. Phenotypic

and immune synapse bioassays support a concurrent restoration of functionality, mostly evident for R-ID, arguably contributing to clinical response.

## INTRODUCTION

The tumor microenvironment (TME) plays a pivotal role in the natural course of chronic lymphocytic leukemia (CLL). This is evidenced by ample immunogenetic cues suggesting selection of the malignant B cell clone by a restricted set of antigens, as well as by the remarkable clinical efficacy of drugs interfering with B-cell receptor signaling (BcR signaling inhibitors, BcRi).[1-6] Although BcRi were developed to target the clonal B cells, accumulating data suggest a pleiotropic effect in the CLL microenvironment, particularly T cells, which may contribute to their clinical efficacy.[7-15]

T cells are intimately implicated in CLL pathophysiology. Xenograft studies have highlighted the importance of trophic signals provided by T cells for the survival of the malignant clone.[16] On the other hand, immunosurveillance by T cells is compromised in CLL, due to, amongst others, defective cytoskeletal signaling and lytic immune synapse formation following tumor immunosuppressive signaling.[17-20] Therefore, delineating the mechanisms driving T cell tolerance rather than effective anti-tumor cytotoxic immune responses is highly relevant and could facilitate optimization of immunotherapy for CLL, with the aim of eradicating minimal residual disease.[21, 22]

Studies employing different methodologies have demonstrated the existence of T cell expansions in CLL.[23-27] Recently, we investigated the role of antigenic stimulation in shaping the T cell repertoire in treatment-naive CLL using next-generation sequencing (NGS).[28] Our study confirmed T cell oligoclonality, with major (high-frequency) clonotypes persisting and further expanding overtime as well as

clonotypes shared among different patients, which appeared to be CLL-specific. Overall, these findings pointed towards selection of T cells by CLL-associated antigenic epitopes.

On these grounds, we sought to comprehensively assess the effect of treatment on CLL T cell repertoire dynamics by combining NGS immunogenetics, flow cytometry and immune synapse bioassays, in order to investigate associations of quantitative and/or qualitative changes with the type of treatment and clinical response. Considering recent data about collateral effects of BcRi treatment on T cells,[7-14, 29] we focused on patients receiving ibrutinib (IB) or rituximab-idelalisib (R-ID) which we compared to patients receiving standard chemoimmunotherapy with the fludarabine-cyclophospphamide-rituximab (FCR) regimen.

In sharp contrast to chemoimmunotherapy, BcRi were found to preserve pre-treatment T cell clones. These clones expanded further as treatment continued and clinical response deepened, particularly in the case of R-ID. Repertoire comparisons revealed major clonotypes shared by different CLL patients but very few “public” clonotypes (i.e. also present in other conditions), suggesting selection by conserved CLL-associated epitopes. Moreover, phenotypic and immune synapse bioassays supported a concurrent restoration of T cell functionality with BcRi therapy, mostly evident for R-ID, arguably contributing to clinical response. Taken together, this data provides a rationale for designing combination strategies aiming to boost cytotoxic anti-tumor responses.

## METHODS

### *Patient group*

We analyzed samples from 28 CLL patients treated in two centres (Thessaloniki, Greece; Milan, Italy) with FCR (n=9), IB (n=15), and/or R-ID (n=10). Patients were selected on the basis of sample availability. Demographic and clinicobiological characteristics are provided in **Suppl. Table 1**. For 22 patients, samples were collected over the 1$^{st}$ line of treatment, either FCR or BcRi. For the remaining 6/28 patients, we analyzed samples collected over consecutive lines of treatment (1$^{st}$ line FCR/2$^{nd}$ line IB, n=3; 1$^{st}$ line FCR/2$^{nd}$ line R-ID, n=2; 1$^{st}$ line IB/2$^{nd}$ line R-ID, n=1). In all cases, samples post-treatment initiation were analyzed in relation to a respective pre-treatment initiation sample. In total, we analyzed 98 peripheral blood (PB) samples: (i) for patients who received FCR, we analyzed samples collected pre-treatment (n=9) and at 3 months after the completion of the 6 cycles (n=9, all in complete remission); (ii) for patients who received BcRi, we analyzed samples pre-treatment (n=25), at 3 months (n=25), 9 months (n=17), best clinical response (median 20 months, n=13)] while still on continuous BcRi treatment. Best response timepoint was defined by the attending physician, and corresponded to the maximal duration of BcRi treatment at the time the study was conducted (median time on BcRi treatment: 20 months), with the single exception of a patient who progressed on IB and proceeded to R-ID as 2$^{nd}$ line treatment. This patient was assessed only at the 3-month timepoint while on IB, at which he had achieved PR. Also, we included 6 bone marrow (BM) samples, collected along with the respective PB pre-treatment sample. A schematic representation of study cohort is provided in **Figure 1A**.

No patient had evidence of infection at sampling. All patients were negative for HBV DNA, anti-HCV and anti-HIV I/II. We carefully excluded patients who developed rituximab-related late-onset neutropenia (R-LON), as it is known to be mediated by cytotoxic T cell clones.[30] The local Ethics Review Committee approved the study and written informed consent form was obtained from all individuals in accordance with the Declaration of Helsinki.

***Next-generation sequencing, definitions and interpretation***

TRBV-TRBD-TRBJ gene rearrangements were RT-PCR amplified and subjected to paired-end NGS (MiSeq, Illumina), as previously described.[28] For all samples, the starting absolute T cell count exceeded $0.5x10^6$ cells to ensure adequate repertoire profiling depth.

Paired-end protocol allowed sequencing of the TRB complementarity-determining region 3 (CDR3) twice/read, thus increasing the accuracy of results. In order to further increase the accuracy of results, raw reads were processed through a purpose-built bioinformatics pipeline performing: (i) length/quality filtering of raw reads; (ii) merging of filtered-in paired reads via local alignment; (iii) length/quality filtering of stitched sequences.[28] Detailed length, quality and overlap rules are provided in **Suppl. Table 2**. Importantly, no base calls of Q-score<30 were allowed in the 75 nucleotide stretch preceding the FGXG motif at the start of TRB FR4, thus further increasing the CDR3 sequencing reliability. Filtered-in sequences were submitted to IMGT/HighV-QUEST (http://www.imgt.org), and metadata was processed by a validated bioinformatics algorithm designed for clonotype computation and repertoire analysis **(Figure 1B)**.[28, 31] Only productive, in-frame

TRBV-TRBD-TRBJ gene rearrangements with functional TRBV genes were included in the analysis. TRBV-TRBD-TRBJ gene rearrangements carrying TRBV genes with <95% germline identity were also discarded as sequences with unacceptable error rate, given the lack of somatic hypermutation in T cells.

Clonotypes were computed as unique pairs of TRBV genes and CDR3 amino acid sequences within a sample. Clonotypes were considered expanded when they contained ≥2 sequences, otherwise they were considered as "singletons". The 10 most expanded clonotypes within a sample are referred to as "major". The relative frequency of each clonotype/sample was calculated as the number of rearrangements corresponding to the clonotype divided by the total number of productive, filtered-in rearrangements for that particular sample.

For TRB gene repertoire analysis, clonotypes rather than single rearrangements were considered in order to avoid potential biases due to expansion following antigenic stimulation, i.e. individual TRBV gene frequencies within a sample were calculated as the number of clonotypes using particular TRBV genes over the total number of clonotypes. Each category of samples (PBMCs, BM) was analyzed separately.

***Inter-patient and across entities clonotype comparison***

We determined the major clonotypes of all CLL samples included in the study (n=563 unique clonotypes, i.e. 10 major clonotypes of each sample removing duplicate values such as clonotypes which persisted in overtime analysis of the same patient or clonotypes shared among different patients) and compared them across CLL patients of this cohort, and against: (i) all T cell clonotypes from our previous NGS study involving treatment-naive CLL patients (n=1,105,728),[28] (ii) T cell clonotypes

from 15 healthy donors (NGS study by our group, n=573,651),[32] (iii) HHV-4 (Ebstein-Barr virus, EBV), HHV-5 (cytomegalovirus, CMV), and BK virus-specific T cell clonotypes (anti-viral T cell NGS study by our group, n=169,502),[33] (iv) non-redundant, well-annotated, unique T cell clonotypes retrieved from public databases (n=17,024),[34, 35] and (v) T cell clonotypes from previous low-throughput immunoprofiling studies (classic subcloning followed by Sanger sequencing) in clinical monoclonal B cell lymphocytosis (high-count MBL, n=545),[36] as well as clinical entities associated with clonal T cell expansions [R-LON (n=283),[30] chronic idiopathic neutropenia (CIN, n=576),[37] large granular T cell leukemia (T-LGL, n=932)].[38-40]

***Flow cytometry***

Multi-color flow cytometry (FACSCanto II cell analyzer, BD Biosciences) was performed to investigate the expression of activation and exhaustion markers (CD25, CD38, CD69, HLA-DR and PD1, respectively) in functionally distinct T cell subpopulations, namely: (i) $CD4^+$ and $CD8^+$ naive T cells ($CD45RA^+/CCR7^+$), (ii) $CD4^+$ and $CD8^+$ central memory T cells (CM, $CD45RO^+/CCR7^+$), (iii) $CD4^+$ and $CD8^+$ effector memory T cells (EM, $CD45RO^+/CCR7^-$), and (iv) $CD4^+$ and $CD8^+$ terminal effector memory RA cells (TEMRA, $CD45RA^+/CCR7^-$). Eight patients (R-ID, n=4; IB, n=4) pre-treatment and at the 3-month timepoint were analyzed, as shown in **Figure 1A**.

Viably frozen peripheral blood mononuclear cells were thawed and resuspended in PBS ($15 \times 10^6$ cells in 1 mL) and incubated with pretitrated Abs to cell-surface markers at 4°C for 20 minutes. CD45 V500, CD3 V450, CD4 PerCP, CD4 PE-Cy7, CD8 PE-Cy7, CCR7 APC-Cy7, CD45RO FITC, CD45RA FITC, CD69 PE, CD25 APC, CD38 PerCP, HLA-DR PE and PD1 APC were used (BD Biosciences). Live lymphocytes were gated

by forward and side scatter, CD45 positive plus 7AAD negative staining. Data were analyzed using the Kaluza flow cytometry analysis software (Beckman Coulter) (**Suppl. Fig. 1**).

An acquisition cut-off of 20,000 $CD3^+$ live cells/sample was applied to ensure reliable representation of all studied T cell subpopulations, as well as uniformity across samples. For T cell activation/exhaustion analysis, results were expressed as the proportion of cells expressing antigens of interest (percent positive staining).

***Immune synapse bioassays, confocal microscopy and quantitative image analysis***

Tumor cell-T cell conjugate assays were designed to test the ability of CLL T cells to form immune synapses with autologous tumor cells. Negatively selected viable CD3+ T cells ($1x10^6$) from untreated, FCR- or BCRi-treated patients were conjugated with equal numbers of autologous CLL tumor cells acting as antigen presenting cells pulsed with super-antigen cocktail and stained with CMAC blue dye (ThermoFisher Scientific) according to the manufacturer's instructions. Cell conjugates were incubated for 15min at 37°C, 5% $CO_2$. Immunofluorescent labeling was done using Cytofuge2 cell concentrator, as described previously.[19] Antibodies (Abs) for rhodamine phalloidin (F-actin staining) and perforin (Alexafluor 488 conjugated) were applied for 45 minutes at 4°C in 5% goat serum (Sigma-Aldrich) solution. After washing, cell specimens were sealed with 22×32 mm coverslips using fluorescent mounting (Dako). Images were captured with an A1R confocal microscope (Nikon) using a 63× oil objective with NIS- Elements software Version 5.01 imaging software (Nikon) and fluorescence was acquired sequentially. The specificity of staining was optimized using isotype-control Abs. Blinded confocal images (n=3 per treatment

group) were analyzed using NIS-Elements software Version 5.01 to measure the F-actin (red fluorescent channel) and perforin (green fluorescent channel) polarization at contact sites and immune synapses using relative recruitment index (RRI) analysis. RRI is calculated as the ratio of F-actin/perforin mean fluorescent intensity at the immune synapse area to the respective value at a cellular membrane area not involved in an immune synapse (RRI<1 indicates a non-polarized, dysfunctional immune synapse). RRI values were expressed as mean value +/- SEM.

***Statistical analysis and visualization tools***

Descriptive statistics for discrete parameters included counts and frequency distributions. The significance of bivariate/multivariate relationships between variables was assessed using the Student t-test, as well as the non-parametric Wilcoxon (for paired values) and Mann-Whitney tests. For all comparisons a significance level of p=0.05 was set.

By applying the Wilcoxon-signed rank test for matched pairs, the power of the NGS analysis ranges from 92% (for the most populated comparison, i.e. pre-IB versus IB at 3 months, n=15 samples) to 53% for the least populated comparisons, i.e. pre-R-ID, R-ID at 3 months, R-ID at 9 months versus R-ID at best response, n=5 samples). A table with power values for each paired comparison is provided in Supplemental Material (**Suppl. Table 3)**.

All statistical analyses were performed using the statistical Package GraphPad Prism version 5.03 (GraphPad Software, Inc., San Diego, USA). For data visualization, either publicly available software (http://circos.ca, https://CRAN.R-project.org) or purpose-built R-tools were utilized.

***Data Sharing Statement***

Raw sequence data have been submitted to the Sequence Read Archive (SRA); BioProject ID: PRJNA552792

## RESULTS

### *The T cell repertoire in CLL is skewed both pre- and post-treatment initiation in all treatment subgroups, with clonal expansions*

First, we profiled by NGS the TR gene repertoire in terms of clonality and TRB gene usage. Overall, 23,262,732 TRBV-TRBD-TRBJ sequences were obtained, of which 20,347,768 (87.5%, median 155,479/sample) passed filters and were further analyzed. The median number of distinct clonotypes/sample was 11,420 (range: 2672-54,045); the median number of expanded clonotypes and singletons/sample was 5287 (range: 772-26,501) and 6417 (range: 1500-32,428), respectively.

All CLL patient blood samples showed a T cell oligoclonal profile. The median T cell clonality of all analyzed samples, calculated as the cumulative frequency of the 10 major clonotypes/sample, was 37.5% (range 8.1-70.5%).

Nine TRBV genes accounted for almost half of the total repertoire both pre-treatment and at the 3-month timepoint (46.8% and 47.6% of the total repertoire, respectively). The relative frequency of each gene did not particularly differentiate over treatment, nor amongst treatment groups (FCR, IB, R-ID)(**Suppl. Figure 2A**). The single exception concerned the TRBV28 gene, which was underrepresented in the R-ID group both pre-treatment and at the 3-month timepoint [3.0%/3.4% versus 5.1%/5.1% in the FCR group ($p<0.01$) versus 4.5%/4.6% in the IB group ($p<0.01$), respectively]. For both the IB and the R-ID groups, where the repertoire was studied beyond the 3-month timepoint, the TRBV gene frequency remained relatively stable overtime and with deepening clinical response (**Suppl. Figure 2B**).

In conclusion, the T cell repertoire was skewed in all examined subgroups, with restricted TRB gene usage and significant clonal expansions.

***T cell clonality increases over treatment and may be associated to clinical response***

We then tested clonality dynamics over treatment and explored associations with clinical response. At cohort level (n=28 patients), circulating T cell clonality increased after treatment [median values from 30.3% pre-treatment to 38.8% ($p<0.05$), 41.9% ($p<0.05$) and 46.2% ($p<0.01$) at the 3-month, 9-month, and deepest clinical response timepoint, respectively].

Within different treatment groups, T cell clonality increased at the 3-month timepoint in the case of FCR (from 28.8% to 46.9%, $p<0.05$) and R-ID (from 33.0% to 39.1%, $p<0.01$), but not IB (from 33.3% to 31.2%, p: 0.99). For the IB and R-ID groups, longitudinal analysis over treatment showed a gradual increase of T cell clonality, related to the depth of clinical response, reaching statistical significance in the case of R-ID [from 33.0% pre-treatment to 39.1% at 3 months ($p<0.01$), 46.0% at 9 months ($p<0.01$) and 46.1% at best clinical response (p: 0.13)], but not IB [from 33.3% pre-treatment to 31.2% at 3 months (p: 0.99), 39.1% at 9 months (p: 0.44) and 42.1% at best clinical response (p: 0.17)] (**Figure 2**).

We also performed analyses where clonality definition was modified in order to include a larger proportion of the repertoire (calculated as the cumulative frequency of the 20 or 50 most expanded clonotypes/sample, instead of 10). These analyses, as well as plots of clonotype frequency in relation to its rank in the repertoire, showed that the gradual increase of clonality resulted from the expansion of the major clonotypes, further alluding to their clinicobiological relevance (**Suppl. Figure 3**).

***Differential impact of chemoimmunotherapy versus BcRi on the T cell repertoire***

To further study clonal dynamics over treatment, we evaluated clonal persistence overtime for each treatment group. We found that chemoimmunotherapy (FCR) resulted in T cell repertoire renewal through ablation and immune reconstitution, whereas BcRi retained most major pre-treatment T cell clones (median number of major pre-treatment clonotypes that persisted at the 3-month timepoint: 2/10 for FCR versus 8/10 for IB versus 7/10 for R-ID) (**Figure 3A**). Overlap analysis of the total repertoire pre- and post-treatment per group showed similar results (**Figure 3B**). Furthermore, in the case of BcRi where the repertoire was studied longitudinally over treatment, repertoire preservation persisted over time (**Figure 3C**).

***Clonotype comparisons document the existence of 'disease-biased' T cell clonotypes***

To obtain insight into the antigenic specificities of the expanded T cell clones, we next listed all unique major clonotypes from our cohort (n=563 clonotypes) and compared them (i) across patients, and (ii) against T cell clonotypes from various entities, as detailed in the Methods section.

Thirty-two of the 563 clonotypes were shared among different CLL patients (**Suppl. Table 4** ), while 18/563 were found in another entity and/or healthy donors ("public" clonotypes") (**Figure 4**). In particular, "public" clonotypes corresponded to 9 matches with T cell clonotypes of herpes virus specificity (CMV, EBV), 2 matches with clonotypes of herpes virus specificity (EBV) that were also found in patients with CIN, and 5 matches with T cell clonotypes from healthy donors. Importantly, of the 32 major clonotypes that were shared among CLL patients, only 9 were "public",

whereas the remaining 23 (23/563, 4.1% of all major clonotypes of our cohort) were shared exclusively by CLL patients, alluding to selection by CLL-associated antigens ("CLL-specific"). Of these 23 “CLL-specific” clonotypes, 3 were shared among 4 different patients, 5 among three different patients, and the remaining 15 among pairs of patients.

***Major CLL-specific T cell clonotypes expand further over treatment***

Considering the above, we repeated our clonality analysis excluding all "public" clonotypes, with similar results. More specifically, clonality significantly increased at the 3-month timepoint in the case of FCR (from 20.8% to 46.9%, $p<0.01$) and R-ID (from 32.9% to 38.8%, $p<0.01$), but not IB (from 33.3% to 31.2%, $p=0.50$). Overtime, clonality increased in both the R-ID and IB group, however reaching statistical significance only in the former [R-ID: from 32.9% to 38.8% at 3 months ($p<0.01$), 44.4% at 9 months ($p<0.01$) and 39.5% at best clinical response (p:ns); IB: from 33.3% to 31.2% at 3 months (p:ns), 39.1% at 9 months (p:ns) and 42.1% at best clinical response (p:ns)] (**Figure 5**).

***Pre-treatment major T cell clonotypes from the peripheral blood are also found in the bone marrow***

For 6 patients (R-ID, n=3 and IB, n=3), synchronous pre-treatment PB and infiltrated BM samples were available. We performed pairwise comparison of the T cell repertoires, to investigate for the presence of PB major clonotypes within the respective BM repertoire. Excluding "public" clonotypes, all PB major clonotypes of

these patients (n=56) were identified within the respective BM repertoires, and 37/56 (66.0%) were listed among the major clonotypes/BM sample.

***Idelalisib-based therapy increases the expression of activation markers on effector memory T cells***

NGS immunoprofiling showed that T cell clonality increased with BcRis, with major clones persisting and further expanding over time. In some cases, these clones were shared among different CLL patients but not found in other entities, suggesting that they may have developed in response to CLL-specific antigens. Therefore, we next wanted to investigate the impact of treatment on T cell functionality, so as to uncover a possible link between these T cell expansions and anti-tumor responses that could contribute to the deepening of clinical response.

To this end, we examined distinct T cell subsets of 8 patients (R-ID, n=4; IB, n=4) pre-treatment and at 3 months for the expression of activation and exhaustion markers by flow cytometry. While the relative frequencies of these T cell subsets, namely $CD4^+$ and $CD8^+$ naive, central memory (CM), effector memory (EM) and terminal effector memory (TEMRA) T cells, did not significantly fluctuate over treatment (data not shown), the expression of activation markers significantly increased post-treatment in the R-ID group compared to the IB group. More specifically, we noted increased expression of: (i) CD69 in $CD4^+$ EM (median fold change 2.0 versus 0.5, $p<0.01$); (ii) CD25 in $CD8^+$ TEMRA (median fold change 1.3 versus 0.5, $p<0.01$), and (iii) CD38 in $CD8^+$ EM (median fold change 1.6 versus 0.3, $p<0.05$) and TEMRA T cells (median fold change 1.1 versus 0.3, $p<0.05$) (**Suppl. Figure 4**).

***BcRi treatment improves T cell immune synapse formation with tumor cells***

Given that T cell dysfunction in CLL has been linked to impaired immune synapse formation, we finally investigated the impact of therapy on immune function by characterizing the ability of patient T cells to form synapse interactions with autologous baseline CLL cells in 13 patients pre-treatment and at 3 months (FCR, n=3; R-ID, n=5; IB, n=5). Confocal microscopy with quantitative image analysis showed that T cells from FCR-treated patients did not improve their ability to form synapse interactions (**Figure 6A**) whereas both BcRi increased the formation of polarized F-actin immune synapses with tumor cells (R-ID, IB, $p<0.05$; FCR, $p=0.99$) (**Figure 6B and C**). We also detected enhanced polarization of the cytolytic molecule perforin towards tumor cells in IB-associated T cell synapses ($p<0.05$) (**Figure 6B**). For 2 patients (R-ID, n=1; IB, n=1), RRI immune synapse analysis was also performed at the deepest clinical response timepoint. These assays revealed no change in T cell synapse formation at the deepest response timepoint reached with IB therapy (25 months) compared to the 3 month timepoint, that may suggest a normalization of T cell function. In contrast, for the patient who received R-ID, deeper clinical response (12 months) correlated with a further increase in polarized immune synapse function (**Figure 6D**).

## DISCUSSION

In the present work we sought to investigate the effect of different types of treatment on T cells from CLL patients. Given the pleiotropic impact of BcRi on the CLL microenvironment, we focused on BcRi as currently used for CLL treatment (IB and R-ID) and compared with standard chemoimmunotherapy (FCR).[13] Our study cohort was significantly enriched for CLL cases with unmutated IGHV genes, the main reason being that these cases are most frequently in need of treatment, especially BcRis. While it cannot directly account for IGHV-mutated CLL, all reported findings concern pair-matched samples (samples of the same patient over time), therefore we argue that IGHV mutational status is not an influent.

We report that T cell clonality significantly increased after treatment with FCR and over treatment with R-ID, and, at least in the case of R-ID, this correlated with the depth of clinical response, peaking at 9 months. A similar trend was detected with IB therapy, however an increase in clonality occurred later in the course of treatment (≥9mo) and did not reach statistical significance, possibly due to the smaller number of samples at more advanced timepoints.

At first glance, the IB results may seem contradictory to a recent study by Yin et al, reporting that IB therapy resulted in TR repertoire diversification, however, certain experimental and analytical differences may explain this.[7] From the start, the use of different clonotype definitions renders the results incomparable: Yin et al reported outcomes on the 1000 most frequent clonotypes (defined as productive unique sequences per sample), while in the present study we focused on the 10 most frequent clonotypes, defined on the basis of unique amino acid CDR3 sequence and

the same IGHV gene. Moreover, Yin et al[7] utilized the ImmunoSEQ platform by Adaptive Biotechnologies, whereas we applied customized, purpose-built bioinformatics algorithms with intentionally strict length and quality filtering. Of note, the increasing T cell repertoire diversity reported by Yin mostly results from an increasing number of singletons. When we performed the same type of analysis in our cohort, following clonotype definition as per the Yin et al study, we also found an increase of the singleton fraction at the 9-month timepoint, although not reaching statistical significance. Besides, Yin et al[7] mention that 6/16 dominant TRBV-TRBJ usages persist and further expand over 12 months of IB therapy, and therefore speculate antigenic stimulation, in an analogy to our results. Finally, Yin et al[7] comment on repertoire diversity by focusing on the emergence of new low-frequency clones over treatment, while, we, on the other hand, focus on the dynamics of the most frequent clones on the consideration that these are the most biologically relevant, and dwell into the hypothesis that may have expanded in response to tumor antigens. We do not comment on repertoire diversity; this may be associated with infectious risks and complications, as hypothesized by Yin et al, but is most probably irrelevant to the dynamics of anti-tumor clones.

Somewhat expectedly, FCR increased T cell clonality through repertoire ablation and reconstitution, probably reflecting a lymphotoxic effect that is restored overtime. Indeed, in a patient who received FCR and was studied prospectively, the increase of clonality at 3 months post-treatment was restored to pre-treatment levels by 9 months. In sharp contrast, BcRi did not reconstitute the T cell repertoire, retaining pre-treatment major T cell clones during therapy, and this was shown consistently for the longest follow-up period reported so far (median 20 months).

In order to obtain evidence as to whether the herin identified T cell clones might have expanded in response to CLL-associated antigens or not, we performed extensive comparisons against not only CLL/MBL sequence datasets,[36, 41] but also datasets from common herpes virus infections (CMV/EBV), healthy individuals, and entities mediated by T cell clones.[30, 32-35, 37-40] and found a significant number of major T cell clonotypes shared exclusively among CLL patients. This is remarkable given: (i) the random HLA background of our cohort, and (ii) the size of the comparison dataset (761,968 distinct TRBV-TRBD-TRBJ sequences). Therefore, this finding supports the existence of (neo)epitopes that are conserved across CLL. Along the same line of reasoning, it is worth noting that, for 3 patients studied over sequential lines of treatment, we found major clonotypes prior to 1$^{st}$ line FCR which disappeared at CR following FCR treatment, but re-emerged as major clonotypes at 1$^{st}$ relapse and persisted through 2$^{nd}$ line treatment with BcRi (data not shown).

In order to investigate the functional impact of treatment on CLL T cells, we studied the expression of activation and exhaustion markers on T cells. We found that R-ID upregulates certain activation markers including IL-2 receptor (CD25) in effector memory T cells compared to IB. Although this increase was arithmetically small, one needs to consider the fact that the frequency of each major clone is relatively low; therefore, even though we purposely focused our analysis on well-defined functional T cell subpopulations, the immunophenotypic activation of anti-tumor T cell clones may be "diluted" within the respective subpopulation. It is also possible that CLL T cells undergo phenotypic changes within tissue TMEs as well as the PB.[42]

Considering that T cell dysfunction in CLL manifests in a defective ability to form immune synapses with tumor B cells, we investigated the effect of treatment on

immune synapse formation capability.[18, 19] We found that, in contrast to FCR, BcRi improved immune synapse function and the recognition of tumor B cells. Interestingly, for the R-ID case which was studied beyond 3 months, this synapse restoration correlated with the depth of clinical response, however definite conclusions cannot be drawn as this was a single case. Improvement in immune synapse formation could be attributed to treatment-induced reduction in tumor load (as the T cell defect has been shown to be tumor-induced)[18, 19]; however, the fact that this did not occur following FCR, the only treatment that led to complete remissions, argues in favor of a BcRi-specific effect on T cell function. Admittedly, the number of cases analyzed for immune synapse formation was limited, due to the substantial number of T cells required for all assays performed in this study. Notably, our results are in keeping with a previous report studying the immunomodulatory impact of FCR and R-IB.[43]

Overall, NGS immunogenetics showed that BcRi retain T cell clones which can expand in parallel to deepening clinical response and possibly contribute to it. This is further corroborated by phenotypic and functional bioassays that demonstrate concurrent T cell activation and improvement in synapse recognition of tumor cells. Taken together, this study provides a rationale for designing future combinatorial therapeutic strategies aiming to boost anti-tumor immune responses. In support of this, recent studies have described the ability of both ibrutinib and idelalisib to enhance chimeric antigen receptor T-cell efficacy in CLL.[44, 45] Future identification of the relevant CLL-associated antigens may eventually pave the way for stratified treatments by means of engineered T cells or peptide vaccines, especially if these epitopes are conserved among CLL patients.

**ACKNOWLEDGMENTS**

Supported in part by ERANET Transcan-2, Project Acronym: Novel, and the Hellenic Precision Medicine Network in Oncology. AV is recipient of a research fellowship from the European Hematology Association (EHA Physician Scientist Research Grant). We thank Theodoros Moysiadis for providing statistical assistance and Tsagiopoulou Maria for providing assistance with fishplot visualizations.

## REFERENCES


1. Fais F, Ghiotto F, Hashimoto S, Sellars B, Valetto A, Allen SL *et al.* Chronic lymphocytic leukemia B cells express restricted sets of mutated and unmutated antigen receptors. *The Journal of clinical investigation* 1998; **102**(8)**:** 1515-1525. doi: 10.1172/JCI3009

2. Damle RN, Wasil T, Fais F, Ghiotto F, Valetto A, Allen SL *et al.* Ig V gene mutation status and CD38 expression as novel prognostic indicators in chronic lymphocytic leukemia. *Blood* 1999; **94**(6)**:** 1840-1847.

3. Stamatopoulos K, Belessi C, Moreno C, Boudjograh M, Guida G, Smilevska T *et al.* Over 20% of patients with chronic lymphocytic leukemia carry stereotyped receptors: Pathogenetic implications and clinical correlations. *Blood* 2007; **109**(1)**:** 259-270. doi: 10.1182/blood-2006-03-012948

4. Agathangelidis A, Darzentas N, Hadzidimitriou A, Brochet X, Murray F, Yan XJ *et al.* Stereotyped B-cell receptors in one-third of chronic lymphocytic leukemia: a molecular classification with implications for targeted therapies. *Blood* 2012; **119**(19)**:** 4467-4475. doi: 10.1182/blood-2011-11-393694

5. Brown JR, Byrd JC, Coutre SE, Benson DM, Flinn IW, Wagner-Johnston ND *et al.* Idelalisib, an inhibitor of phosphatidylinositol 3-kinase p110delta, for relapsed/refractory chronic lymphocytic leukemia. *Blood* 2014; **123**(22)**:** 3390-3397. doi: 10.1182/blood-2013-11-535047

6. Byrd JC, Furman RR, Coutre SE, Flinn IW, Burger JA, Blum KA *et al.* Targeting BTK with ibrutinib in relapsed chronic lymphocytic leukemia. *The New England journal of medicine* 2013; **369**(1)**:** 32-42. doi: 10.1056/NEJMoa1215637

7. Yin Q, Sivina M, Robins H, Yusko E, Vignali M, O'Brien S *et al.* Ibrutinib Therapy Increases T Cell Repertoire Diversity in Patients with Chronic Lymphocytic Leukemia. *Journal of immunology* 2017; **198**(4)**:** 1740-1747. doi: 10.4049/jimmunol.1601190

8. Niemann CU, Herman SE, Maric I, Gomez-Rodriguez J, Biancotto A, Chang BY *et al.* Disruption of in vivo Chronic Lymphocytic Leukemia Tumor-Microenvironment Interactions by Ibrutinib--Findings from an Investigator-Initiated Phase II Study. *Clinical cancer research : an official journal of the American Association for Cancer Research* 2016; **22**(7)**:** 1572-1582. doi: 10.1158/1078-0432.CCR-15-1965

9. Dubovsky JA, Beckwith KA, Natarajan G, Woyach JA, Jaglowski S, Zhong Y *et al.* Ibrutinib is an irreversible molecular inhibitor of ITK driving a Th1-selective pressure in T lymphocytes. *Blood* 2013; **122**(15)**:** 2539-2549. doi: 10.1182/blood-2013-06-507947

10. Ali K, Soond DR, Pineiro R, Hagemann T, Pearce W, Lim EL *et al.* Inactivation of PI(3)K p110delta breaks regulatory T-cell-mediated immune tolerance to cancer. *Nature* 2014; **510**(7505)**:** 407-411. doi: 10.1038/nature13444

11. Herman SE, Gordon AL, Wagner AJ, Heerema NA, Zhao W, Flynn JM *et al.* Phosphatidylinositol 3-kinase-delta inhibitor CAL-101 shows promising preclinical activity in chronic lymphocytic leukemia by antagonizing intrinsic and extrinsic cellular survival signals. *Blood* 2010; **116**(12)**:** 2078-2088. doi: 10.1182/blood-2010-02-271171

12. Lampson BL, Kasar SN, Matos TR, Morgan EA, Rassenti L, Davids MS *et al.* Idelalisib given front-line for treatment of chronic lymphocytic leukemia causes frequent immune-mediated hepatotoxicity. *Blood* 2016; **128**(2)**:** 195-203. doi: 10.1182/blood-2016-03-707133

13. Maharaj K, Sahakian E, Pinilla-Ibarz J. Emerging role of BCR signaling inhibitors in immunomodulation of chronic lymphocytic leukemia. *Blood advances* 2017; **1**(21)**:** 1867-1875. doi: 10.1182/bloodadvances.2017006809

14. Dong S, Guinn D, Dubovsky JA, Zhong Y, Lehman A, Kutok J *et al.* IPI-145 antagonizes intrinsic and extrinsic survival signals in chronic lymphocytic leukemia cells. *Blood* 2014; **124**(24)**:** 3583-3586. doi: 10.1182/blood-2014-07-587279

15. Long M, Beckwith K, Do P, Mundy BL, Gordon A, Lehman AM *et al.* Ibrutinib treatment improves T cell number and function in CLL patients. *The Journal of clinical investigation* 2017; **127**(8)**:** 3052-3064. doi: 10.1172/JCI89756

16. Bagnara D, Kaufman MS, Calissano C, Marsilio S, Patten PE, Simone R *et al.* A novel adoptive transfer model of chronic lymphocytic leukemia suggests a key role for T lymphocytes in the disease. *Blood* 2011; **117**(20)**:** 5463-5472. doi: 10.1182/blood-2010-12-324210

17. Gorgun G, Holderried TA, Zahrieh D, Neuberg D, Gribben JG. Chronic lymphocytic leukemia cells induce changes in gene expression of CD4 and CD8 T cells. *The Journal of clinical investigation* 2005; **115**(7)**:** 1797-1805. doi: 10.1172/JCI24176

18. Ramsay AG, Johnson AJ, Lee AM, Gorgun G, Le Dieu R, Blum W *et al.* Chronic lymphocytic leukemia T cells show impaired immunological synapse formation that can be reversed with an immunomodulating drug. *The Journal of clinical investigation* 2008; **118**(7)**:** 2427-2437. doi: 10.1172/JCI35017

19. Ramsay AG, Clear AJ, Fatah R, Gribben JG. Multiple inhibitory ligands induce impaired T-cell immunologic synapse function in chronic lymphocytic leukemia that can be blocked with lenalidomide: establishing a reversible immune evasion

mechanism in human cancer. *Blood* 2012; **120**(7)**:** 1412-1421. doi: 10.1182/blood-2012-02-411678

20. Ramsay AG, Evans R, Kiaii S, Svensson L, Hogg N, Gribben JG. Chronic lymphocytic leukemia cells induce defective LFA-1-directed T-cell motility by altering Rho GTPase signaling that is reversible with lenalidomide. *Blood* 2013; **121**(14)**:** 2704-2714. doi: 10.1182/blood-2012-08-448332

21. Shanafelt TD, Ramsay AG, Zent CS, Leis JF, Tun HW, Call TG *et al.* Long-term repair of T-cell synapse activity in a phase II trial of chemoimmunotherapy followed by lenalidomide consolidation in previously untreated chronic lymphocytic leukemia (CLL). *Blood* 2013; **121**(20)**:** 4137-4141. doi: 10.1182/blood-2012-12-470005

22. Ding W, LaPlant BR, Call TG, Parikh SA, Leis JF, He R *et al.* Pembrolizumab in patients with CLL and Richter transformation or with relapsed CLL. *Blood* 2017; **129**(26)**:** 3419-3427. doi: 10.1182/blood-2017-02-765685

23. Farace F, Orlanducci F, Dietrich PY, Gaudin C, Angevin E, Courtier MH *et al.* T cell repertoire in patients with B chronic lymphocytic leukemia. Evidence for multiple in vivo T cell clonal expansions. *Journal of immunology* 1994; **153**(9)**:** 4281-4290.

24. Rezvany MR, Jeddi-Tehrani M, Osterborg A, Kimby E, Wigzell H, Mellstedt H. Oligoclonal TCRBV gene usage in B-cell chronic lymphocytic leukemia: major perturbations are preferentially seen within the CD4 T-cell subset. *Blood* 1999; **94**(3)**:** 1063-1069.

25. Goolsby CL, Kuchnio M, Finn WG, Peterson L. Expansions of clonal and oligoclonal T cells in B-cell chronic lymphocytic leukemia are primarily restricted to the CD3(+)CD8(+) T-cell population. *Cytometry* 2000; **42**(3)**:** 188-195.

26. Zaborsky N, Holler C, Geisberger R, Asslaber D, Gassner FJ, Egger V *et al.* B-cell receptor usage correlates with the sensitivity to CD40 stimulation and the occurrence of CD4+ T-cell clonality in chronic lymphocytic leukemia. *Haematologica* 2015; **100**(8)**:** e307-310. doi: 10.3324/haematol.2015.124719

27. Vardi A, Agathangelidis A, Stalika E, Karypidou M, Siorenta A, Anagnostopoulos A *et al.* Antigen Selection Shapes the T-cell Repertoire in Chronic Lymphocytic Leukemia. *Clinical cancer research : an official journal of the American Association for Cancer Research* 2016; **22**(1)**:** 167-174. doi: 10.1158/1078-0432.CCR-14-3017

28. Vardi A, Vlachonikola E, Karypidou M, Stalika E, Bikos V, Gemenetzi K *et al.* Restrictions in the T-cell repertoire of chronic lymphocytic leukemia: high-throughput immunoprofiling supports selection by shared antigenic elements. *Leukemia* 2017; **31**(7)**:** 1555-1561. doi: 10.1038/leu.2016.362

29. Garcon F, Okkenhaug K. PI3Kdelta promotes CD4(+) T-cell interactions with antigen-presenting cells by increasing LFA-1 binding to ICAM-1. *Immunology and cell biology* 2016; **94**(5)**:** 486-495. doi: 10.1038/icb.2016.1

30. Stamatopoulos K, Papadaki T, Pontikoglou C, Athanasiadou I, Stavroyianni N, Bux J *et al.* Lymphocyte subpopulation imbalances, bone marrow hematopoiesis and histopathology in rituximab-treated lymphoma patients with late-onset neutropenia. *Leukemia* 2008; **22**(7)**:** 1446-1449. doi: 10.1038/sj.leu.2405077

31. Maramis C, Gkoufas A, Vardi A, Stalika E, Stamatopoulos K, Hatzidimitriou A *et al.* IRProfiler - a software toolbox for high throughput immune receptor profiling. *BMC bioinformatics* 2018; **19**(1)**:** 144. doi: 10.1186/s12859-018-2144-z

32. Agathangelidis A, Galigalidou C, Scarfo L, Moysiadis T, Rovida A, Vlachonikola E *et al.* High-throughput analysis of the T cell receptor gene repertoire in low-count monoclonal B cell lymphocytosis reveals a distinct profile from chronic lymphocytic leukemia. *Haematologica* 2020. doi: 10.3324/haematol.2019.221275

33. Gemenetzi K, Galigalidou C, Hadzidimitriou A, Stalika E, Vlachonikola E, Agathangelidis A *et al*. High-Throughput T Cell Receptor (TR) Repertoire Analysis of Virus-Specific T Cells: Implications for T Cell Immunotherapy and Viral Infection Risk Stratification. *ASH Annual Meeting* 2018.

34. Shugay M, Bagaev DV, Zvyagin IV, Vroomans RM, Crawford JC, Dolton G *et al.* VDJdb: a curated database of T-cell receptor sequences with known antigen specificity. *Nucleic acids research* 2018; **46**(D1)**:** D419-D427. doi: 10.1093/nar/gkx760

35. Giudicelli V, Duroux P, Ginestoux C, Folch G, Jabado-Michaloud J, Chaume D *et al.* IMGT/LIGM-DB, the IMGT comprehensive database of immunoglobulin and T cell receptor nucleotide sequences. *Nucleic acids research* 2006; **34**(Database issue)**:** D781-784. doi: 10.1093/nar/gkj088

36. Blanco G VA, Puiggros A, Gomez-Llonin A, Muro M, Rodriguez-Rivera M, et al. Restricted T cell receptor repertoire in CLL-like monoclonal B cell lymphocytosis and early stage CLL. *Oncoimmunology* 2018; **7**(6)**:** e1432328.

37. Mastrodemou S, Stalika E, Vardi A, Gemenetzi K, Spanoudakis M, Karypidou M *et al.* Cytotoxic T cells in chronic idiopathic neutropenia express restricted antigen receptors. *Leukemia & lymphoma* 2017; **58**(12)**:** 2926-2933. doi: 10.1080/10428194.2017.1324154

38. Stalika E, Papalexandri A, Iskas M, Stavroyianni N, Kanellis G, Kotta K *et al.* Familial CD3+ T large granular lymphocyte leukemia: evidence that genetic predisposition

and antigen selection promote clonal cytotoxic T-cell responses. *Leukemia & lymphoma* 2014; **55**(8)**:** 1781-1787. doi: 10.3109/10428194.2013.861065

39. Papalexandri A, Stalika E, Iskas M, Karypidou M, Zerva P, Touloumenidou T *et al.* Molecular evidence for repertoire skewing of T large granular lymphocyte proliferation after allogeneic hematopoietic SCT: report of two cases. *Bone marrow transplantation* 2013; **48**(9)**:** 1260-1261. doi: 10.1038/bmt.2013.40

40. Stalika E, Papalexandri A, Kannelis G, Batsis I, Papadaki T, Anagnostopoulos A *et al.* Transient monoclonal CD3+ T large granular lymphocyte proliferation in a case of mantle cell lymphoma with Rituximab-associated late onset neutropenia. *Hematological oncology* 2011; **29**(3)**:** 144-146. doi: 10.1002/hon.963

41. Derniame S, Vignaud JM, Faure GC, Bene MC, Massin F. Comparative T-cell oligoclonality in lung, tumor and lymph nodes in human non-small cell lung cancer. *Oncology reports* 2005; **13**(3)**:** 509-515.

42. Hanna BS, Roessner PM, Yazdanparast H, Colomer D, Campo E, Kugler S *et al.* Control of chronic lymphocytic leukemia development by clonally-expanded CD8(+) T-cells that undergo functional exhaustion in secondary lymphoid tissues. *Leukemia* 2019; **33**(3)**:** 625-637. doi: 10.1038/s41375-018-0250-6

43. Papazoglou D, Lesnick CE, Wang V, Kay NE, Shanafelt TD, Ramsay AG. Ibrutinib-Based Therapy Improves Anti-Tumor T Cell Killing Function Allowing Effective Pairing with Anti-PD-L1 Immunotherapy Compared to Traditional FCR Chemoimmunotherapy; Implications for Therapy and Correlative Immune Functional Data from the Phase III E1912 Trial. *Blood* 2019; **132**(Suppl. 1)**:** 236. doi: 10.1182/blood-2018-99-118333

44. Fraietta JA, Beckwith KA, Patel PR, Ruella M, Zheng Z, Barrett DM *et al.* Ibrutinib enhances chimeric antigen receptor T-cell engraftment and efficacy in leukemia. *Blood* 2016; **127**(9)**:** 1117-1127. doi: 10.1182/blood-2015-11-679134

45. Stock S, Ubelhart R, Schubert ML, Fan F, He B, Hoffmann JM *et al.* Idelalisib for optimized CD19-specific chimeric antigen receptor T cells in chronic lymphocytic leukemia patients. *International journal of cancer* 2019; **145**(5)**:** 1312-1324. doi: 10.1002/ijc.32201

**FIGURE LEGENDS**

**Figure 1. A. Schematic representation of the study cohort.** The FCR treatment group included 9 patients sampled prior to treatment and 3 months after completion of 6 FCR cycles. The IB group included 15 patients [12 receiving IB as 1st line treatment and 3, coming from the FCR treatment group, who relapsed after FCR and received IB as 2nd line treatment (the latter *in dark grey*)]. The R-ID group included 10 patients [7 receiving R-ID as 1st line treatment, 2 coming from the FCR treatment group who relapsed after FCR and received R-ID as 2nd line treatment (*in light grey without outline*), and 1 coming from the IB treatment group who relapsed on IB and received R-ID as 2nd line treatment (*in light gray with outline*)]. Sampling timepoints for the IB and R-ID treatment groups were 3 months, 9 months and at best clinical response while on continuous BcRi treatment. For 6 patients (*underlined by a dashed line*, IB, n=3; R-ID, n=3), bone marrow samples were also obtained in addition to PB prior to BcRi treatment. All samples were analyzed by NGS. Immune synapse bioassays were performed for 14 patients (*marked with a dot*; FCR, n=3; IB, n=6; R-ID, n=5). Flow cytometry for activation/exhaustion markers was performed for 8 patients (*marked with a light grey dot* IB, n=4; R-ID, n=4). **B. Schematic representation of the NGS pipeline.** TRBV-TRBD-TRBJ gene rearrangements were RT-PCR amplified and subjected to paired-end NGS (MiSeq, Illumina), as previously described.[29] Instead of arbitrarily excluding low-frequency clonotypes, which may lead to underestimation of repertoire diversity, both the read-stiching algorithm as well as IRProfiler apply strict quality rules in order to maximize the accuracy of results.

**Figure 2. T cell clonality significantly increases after treatment with FCR and over treatment with R-ID.** The % cumulative frequency of the major clonotypes is depicted overtime per treatment group in a box-whisker fashion.

**Figure 3. FCR results in T cell repertoire renewal, whereas BcRi treatment retains pre-treatment T cell clones.** Venn diagrams are used to depict the overlap between the T cell repertoire pre-treatment and at the 3-month timepoint per treatment group, concerning **(A)** only the major T cell clonotypes, and **(B)** the total T cell repertoire. Overlap was calculated as the percentage of clonotypes of the pre-treatment repertoire which persisted at 3 months. **(C) The T cell repertoire conservation remains over time for the IB and R-ID group.** The

Jaccard index, defined as the size of the intersection divided by the size of the union of the two sample sets [Jaccard similarity coefficient, J(A,B)=|A∩B|/(|A|+|B|-|A∩B|)], is plotted on the (y) axis. Comparisons concern the repertoire of each patient (dot) pre/3 months, pre/9 months and pre/deepest response, per treatment group. The median overlap (vertical line) remains practically the same over time for the IB and R-ID group, and significantly higher than for FCR.

**Figure 4. "Public" and CLL-specific clonotypes.** Of the 563 major clonotypes of the CLL cohort, 41 (7%) were found in other entities ("public") or shared among different CLL patients ("CLL-specific")

**Figure 5. Clonality analysis overtime, excluding "public" clonotypes. (A) Clonality significantly increases after treatment with FCR and over treatment with R-ID.** The % cumulative frequency of the major clonotypes is depicted overtime per treatment group in a box-whisker fashion, after having excluded clonotypes that were also found in other entities/healthy individuals ("public" clonoypes). **(B) Persisting clonotypes expand overtime, especially in the case of R-ID.** Fishplots depicting how the frequency of each persisting major clonotype changes in relation to the pre-treatment timepoint, again having excluded "public" clonotypes. Three characteristic cases of patients receiving R-ID and IB are depicted in the left and right column, respectively. Each ribbon represents a CLL-specific major clonotype which persists in all three timepoints over treatment (sequentially: pre-treatment, at 3 months, 9 months, and deepest response) and the thickness of the ribbon at each timepoint corresponds to the clonotype's relative frequency. The remaining repertoire is shown in *white* for all cases.

**Figure 6. BcRi treatment restores F-actin immunological synapses between CLL tumor cells and autologous T cells.** Untreated CLL tumor cells (CMAC dyed, blue) were conjugated with autologous negatively selected $CD3^+$ T cells from CLL patient samples obtained prior initiation of treatment (pre) and 3 months post treatment. All conjugates per treatment time-point were acquired using a confocal microscope. Quantitative image analysis (relative recruitment index [RRI]) was used for the calculation of F-actin (red) and perforin (green) polarization towards the tumor cell in T-cell/B-cell conjugates of **(A)** FCR (n=3), **(B)** ibrutinib

(IB) (n=6) and **(C)** R-idelalisib (R-ID) (n=5) treated samples. Bar charts show the mean RRI values of all T-cell/B-cell CLL conjugates per treatment ± SEM. The confocal images show representative T-cell/B-cell conjugates for all treatments. Original magnification of immunofluorescence images ×63. **(D)** F-actin RRI analysis over deepening response for two patients on BcRi. Each dot corresponds to the mean RRI values ± SEM for treatment time-point. Differences between pre- and post-treatment samples were assessed by Wilcoxon signed-rank test. *$p < 0.05$

**Fig. 1**

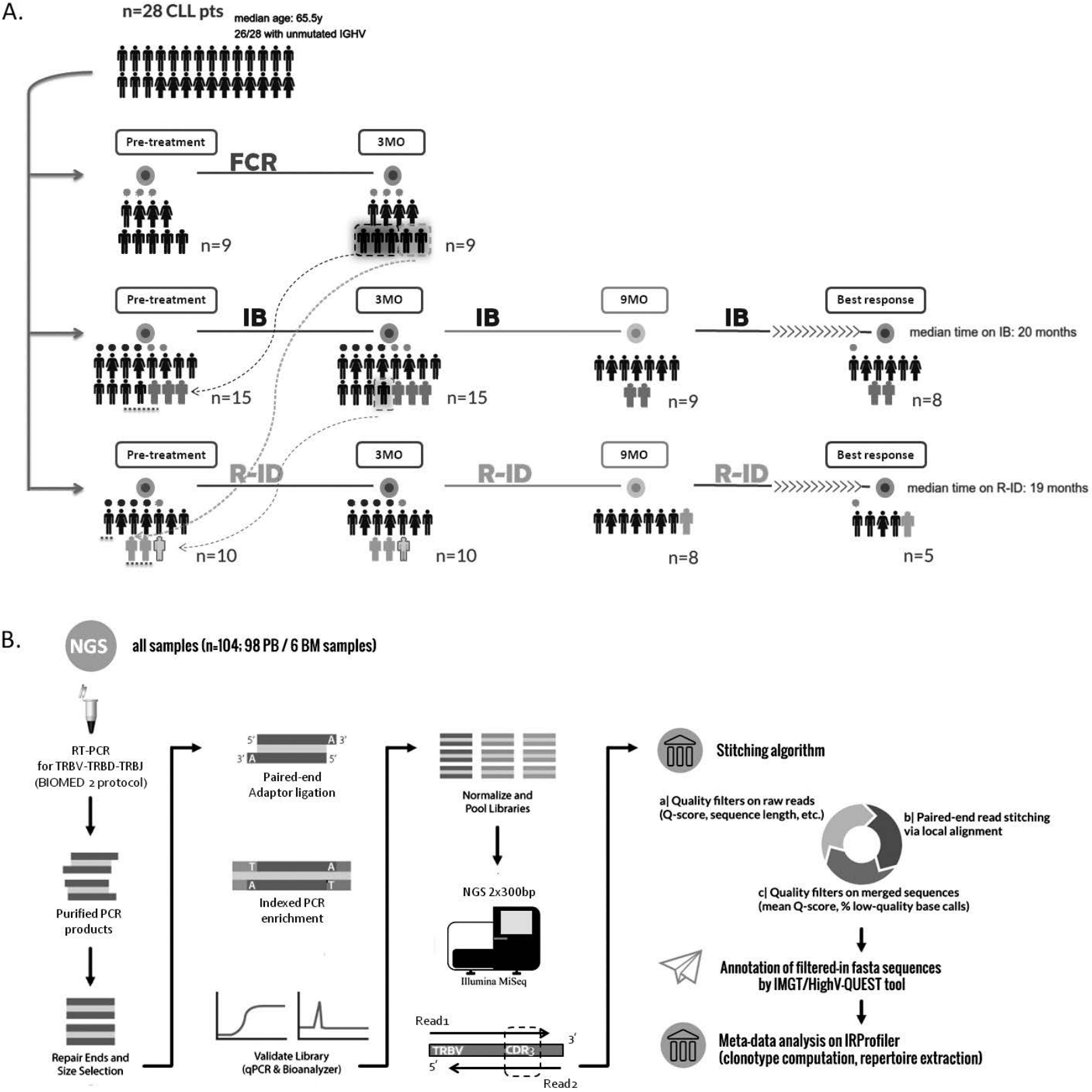
A.
n=28 CLL pts
median age: 65.5y
26/28 with unmutated IGHV
Pre-treatment
FCR
3MO
n=9
n=9
Pre-treatment
IB
3MO
IB
9MO
IB
Best response
median time on IB: 20 months
n=15
n=15
n=9
n=8
Pre-treatment
R-ID
3MO
R-ID
9MO
R-ID
Best response
median time on R-ID: 19 months
n=10
n=10
n=8
n=5
B.
NGS
all samples (n=104: 98 PB / 6 BM samples)
RT-PCR
for TRBV-TRBD-TRBJ
(BIOMED 2 protocol)
Purified PCR
products
Repair Ends and
Size Selection
Paired-end
Adaptor ligation
Indexed PCR
enrichment
Validate Library
(qPCR & Bioanalyzer)
Normalize and
Pool Libraries
NGS 2x300bp
Illumina MiSeq
Read1
TRBV
CDR3
Read2
Stitching algorithm
a| Quality filters on raw reads
(Q-score, sequence length, etc.)
b| Paired-end read stitching
via local alignment
c| Quality filters on merged sequences
(mean Q-score, % low-quality base calls)
Annotation of filtered-in fasta sequences
by IMGT/HighV-QUEST tool
Meta-data analysis on IRProfiler
(clonotype computation, repertoire extraction)

**Fig. 2**

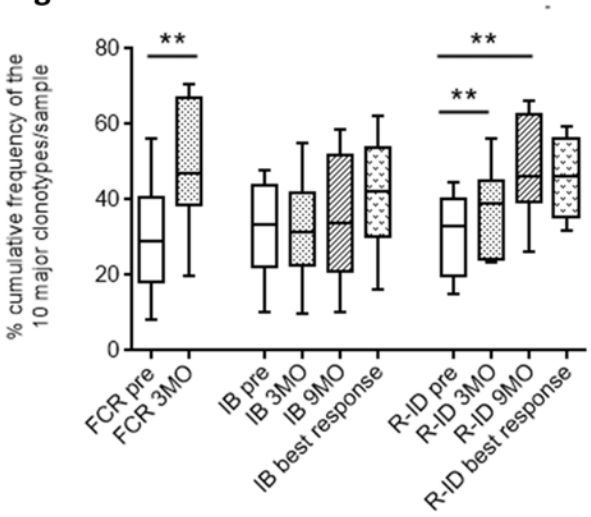
% cumulative frequency of the 10 major clonotypes/sample
80
60
40
20
0
**
**
**
FCR pre
FCR 3MO
IB pre
IB 3MO
IB 9MO
IB best response
R-ID pre
R-ID 3MO
R-ID 9MO
R-ID best response

**Fig. 3A**


pre FCR
FCR 3MO
20%

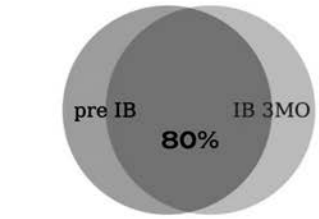
pre IB
IB 3MO
80%

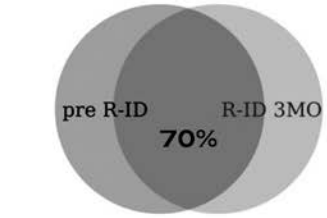
pre R-ID
R-ID 3MO
70%

**Fig. 3B**


pre FCR
FCR 3MO
0.6%

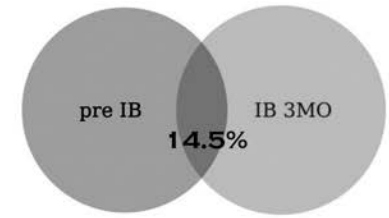
pre IB
IB 3MO
14.5%

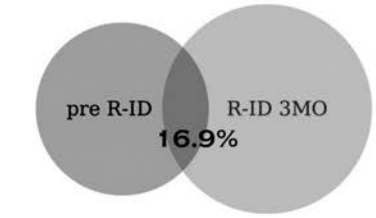
pre R-ID
R-ID 3MO
16.9%

Fig. 3C

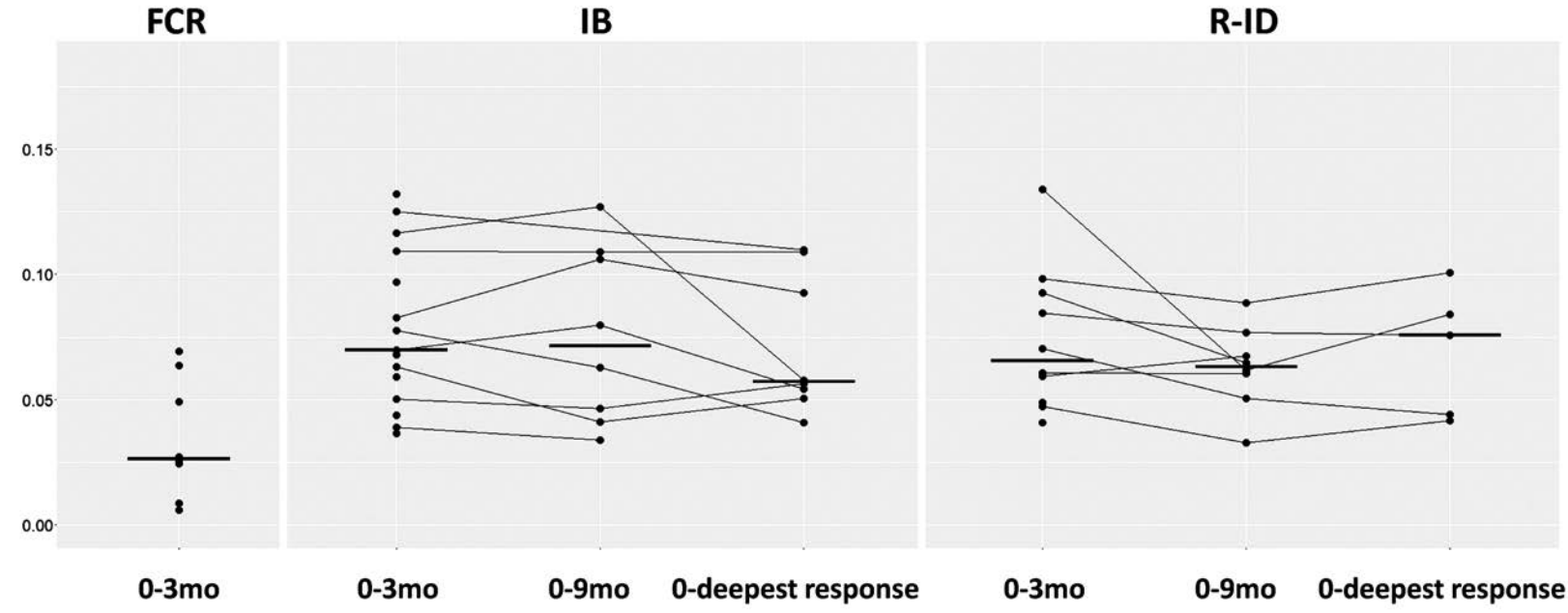
FCR
IB
R-ID
0.15
0.10
0.05
0.00
0-3mo
0-3mo
0-9mo
0-deepest response
0-3mo
0-9mo
0-deepest response

**Fig. 4**

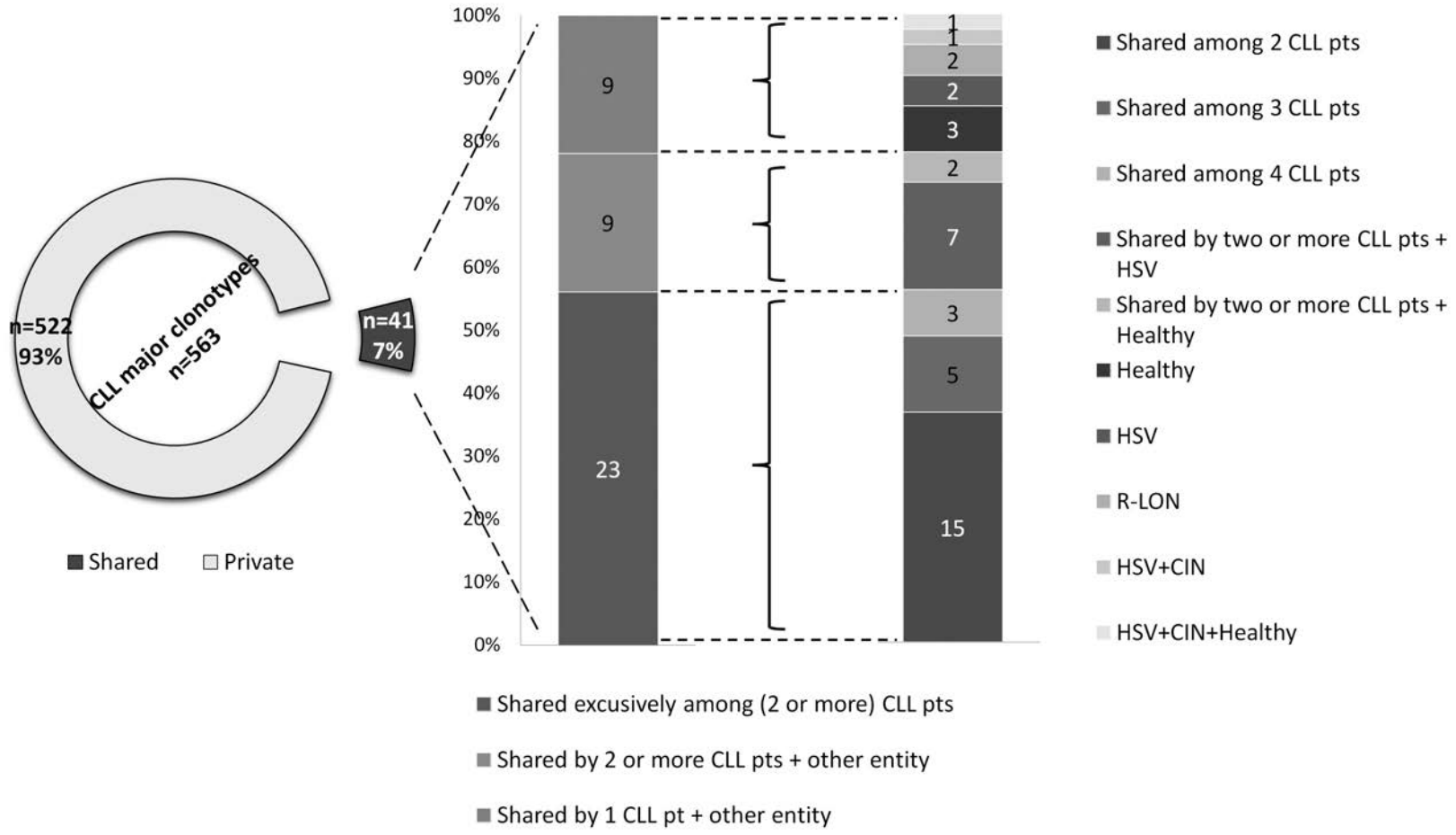
n=522
93%
CLL major clonotypes
n=563
n=41
7%
Shared
Private
100%
90%
80%
70%
60%
50%
40%
30%
20%
10%
0%
9
9
23
1
1
2
2
3
2
7
3
5
15
Shared among 2 CLL pts
Shared among 3 CLL pts
Shared among 4 CLL pts
Shared by two or more CLL pts + HSV
Shared by two or more CLL pts + Healthy
Healthy
HSV
R-LON
HSV+CIN
HSV+CIN+Healthy
Shared excusively among (2 or more) CLL pts
Shared by 2 or more CLL pts + other entity
Shared by 1 CLL pt + other entity

**Fig. 5A**

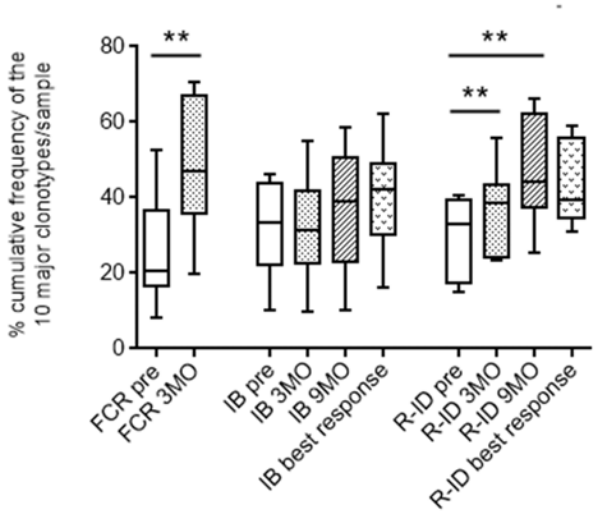
% cumulative frequency of the 10 major clonotypes/sample
80
60
40
20
0
**
**
**
FCR pre
FCR 3MO
IB pre
IB 3MO
IB 9MO
IB best response
R-ID pre
R-ID 3MO
R-ID 9MO
R-ID best response

Fig. 5B

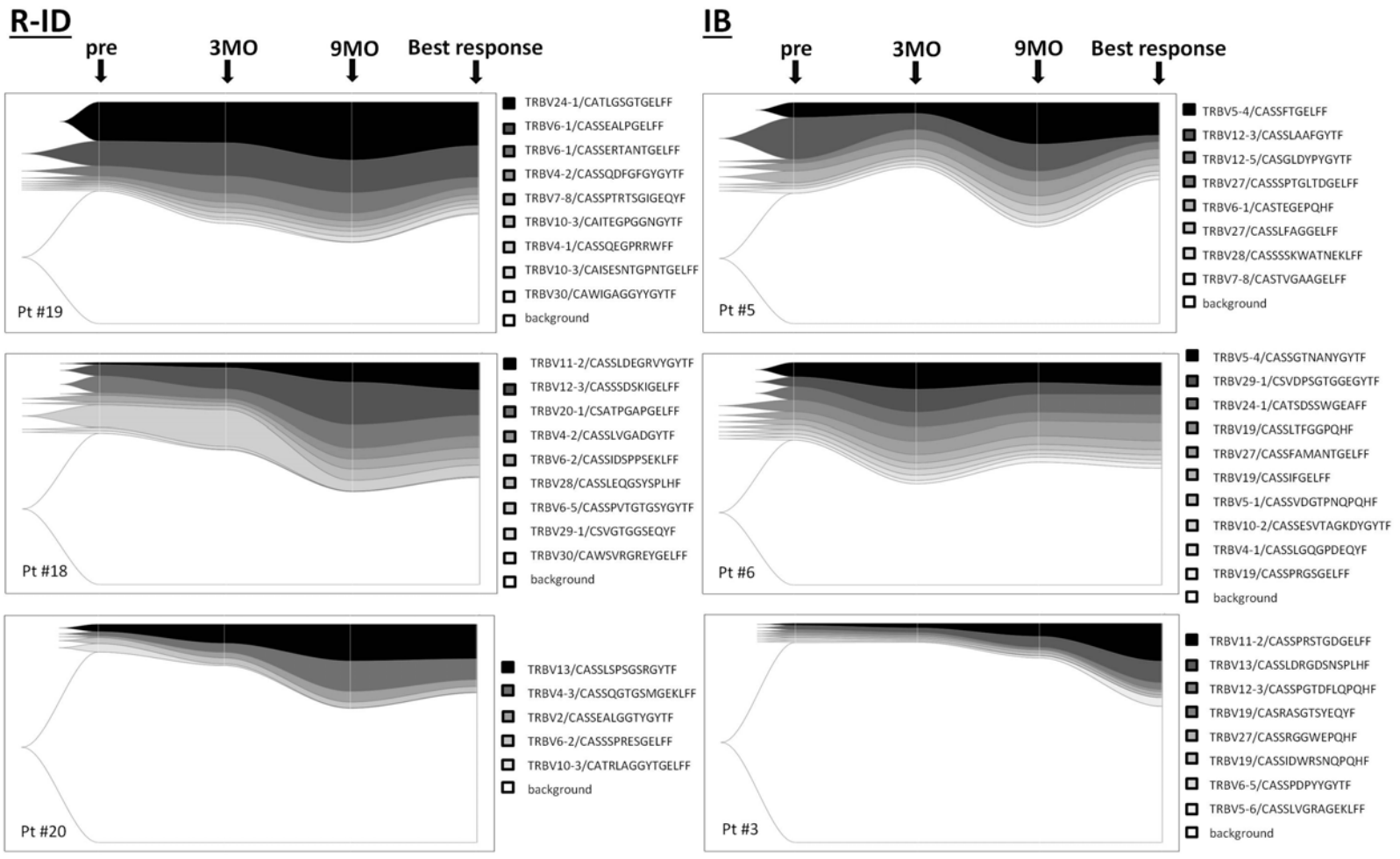
R-ID
pre
3MO
9MO
Best response
TRBV24-1/CATLGSGTGELFF
TRBV6-1/CASSEALPGELFF
TRBV6-1/CASSERTANTGELFF
TRBV4-2/CASSQDFGFGYGYTF
TRBV7-8/CASSPTRTSGIGEQYF
TRBV10-3/CAITEGPGGNGYTF
TRBV4-1/CASSQEGPRRWFF
TRBV10-3/CAISESNTGPNTGELFF
TRBV30/CAWIGAGGYYGYTF
background
Pt #19
TRBV11-2/CASSLDEGRVYGYTF
TRBV12-3/CASSSDSKIGELFF
TRBV20-1/CSATPGAPGELFF
TRBV4-2/CASSLVGADGYTF
TRBV6-2/CASSIDSPPSEKLFF
TRBV28/CASSLEQGSYSPLHF
TRBV6-5/CASSPVTGTGSYGYTF
TRBV29-1/CSVGTGGSEQYF
TRBV30/CAWSVRGREYGELFF
background
Pt #18
TRBV13/CASSLSPSGSRGYTF
TRBV4-3/CASSQGTGSMGEKLFF
TRBV2/CASSEALGGTYGYTF
TRBV6-2/CASSSPRESGELFF
TRBV10-3/CATRLAGGYTGELFF
background
Pt #20
IB
pre
3MO
9MO
Best response
TRBV5-4/CASSFTGELFF
TRBV12-3/CASSLAAFGYTF
TRBV12-5/CASGLDYPYGYTF
TRBV27/CASSSPTGLTDGELFF
TRBV6-1/CASTEGEPQHF
TRBV27/CASSLFAGGELFF
TRBV28/CASSSSKWATNEKLFF
TRBV7-8/CASTVGAAGELFF
background
Pt #5
TRBV5-4/CASSGTNANYGYTF
TRBV29-1/CSVDPSGTGGEGYTF
TRBV24-1/CATSDSSWGEAFF
TRBV19/CASSLTFGGPQHF
TRBV27/CASSFAMANTGELFF
TRBV19/CASSIFGELFF
TRBV5-1/CASSVDGTPNQPQHF
TRBV10-2/CASSESVTAGKDYGYTF
TRBV4-1/CASSLGQGPDEQYF
TRBV19/CASSPRGSGELFF
background
Pt #6
TRBV11-2/CASSPRSTGDGELFF
TRBV13/CASSLDRGDSNSPLHF
TRBV12-3/CASSPGTDFLQPQHF
TRBV19/CASRASGTSYEQYF
TRBV27/CASSRGGWEPQHF
TRBV19/CASSIDWRSNQPQHF
TRBV6-5/CASSPDPYYGYTF
TRBV5-6/CASSLVGRAGEKLFF
background
Pt #3

Fig. 6

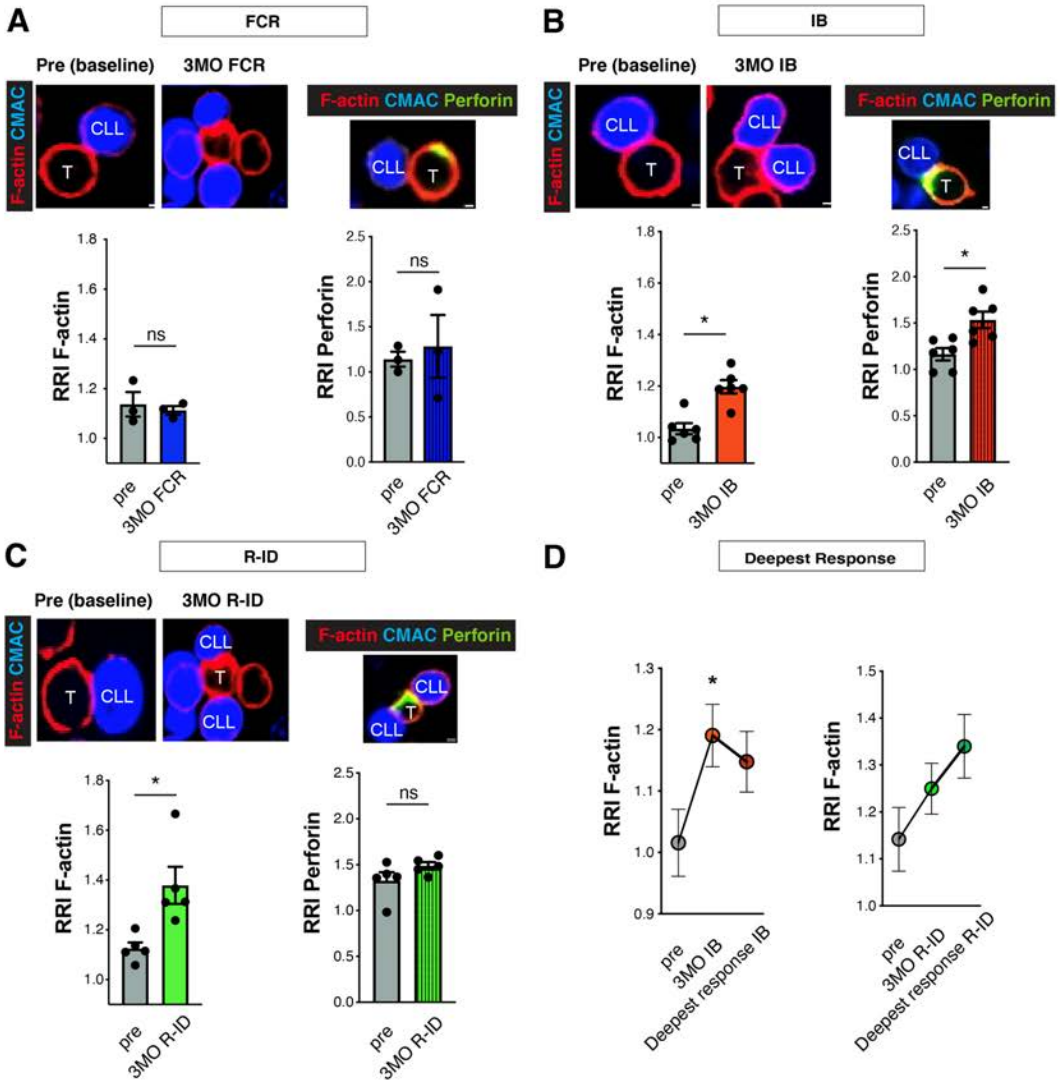
A
FCR
Pre (baseline)
3MO FCR
F-actin CMAC
F-actin CMAC Perforin
CLL
T
RRI F-actin
RRI Perforin
ns
pre
3MO FCR
B
IB
Pre (baseline)
3MO IB
*
3MO IB
C
R-ID
Pre (baseline)
3MO R-ID
3MO R-ID
D
Deepest Response
pre
3MO IB
Deepest response IB
3MO R-ID
Deepest response R-ID

**SUPPLEMENTAL TABLE 1. Study cohort demographics and clinicobiological information**

| Patient ID | Date of birth | Sex | Rai at diagnosis | Binet at diagnosis | Karyotype | FISH del(13q) monoallelic result | FISH del(13q) biallelic result | FISH trisomy 12 result | FISH del(11q) result | FISH del(17p) result | TP53 abnormality | TP53 nucleotide change | NOTCH1 mutation result | IGHV | IGHD | IGHJ | IGHV GI Identity % |
|---|---|---|---|---|---|---|---|---|---|---|---|---|---|---|---|---|---|
| Patient 1 | 15/08/1966 | M | I | A | 46,XY[20] | NEGATIVE | NEGATIVE | NEGATIVE | NEGATIVE | NEGATIVE | NEGATIVE | | NEGATIVE | IGHV2-5*01 | IGHD3-3*02 | IGHJ4*02 | 100.00 |
| Patient 2 | 16/05/1952 | M | II | B | 46,XY, del(17)(p13)[3]/45, X,-Y[3]/46,XY[24] | | | | | POSITIVE | POSITIVE | A536G | NEGATIVE | IGHV5-51*01 | IGHD2-2*01 | IGHJ4*01 | 100.00 |
| Patient 3 | 01/01/1953 | F | II | B | 46,XX,t(14;22)(q34;q11)[6]/46XX[22] | NEGATIVE | NEGATIVE | NEGATIVE | NEGATIVE | POSITIVE | | | | IGHV3-48*02 | IGHD1-26*01 | IGHJ1*01 | 98.96 |
| Patient 4 | 22/07/1952 | M | I | A | | NEGATIVE | NEGATIVE | NEGATIVE | NEGATIVE | NEGATIVE | NEGATIVE | | NEGATIVE | IGHV1-69*04 | IGHD3-10*01 | IGHJ6*02 | 100.00 |
| Patient 5 | 24/04/1948 | F | IV | C | 46,XX[20] | POSITIVE | NEGATIVE | NEGATIVE | NEGATIVE | NEGATIVE | NEGATIVE | | NEGATIVE | IGHV3-30-3*01 | IGHD3-10*01 | IGHJ4*02 | 100.00 |
| Patient 6 | 05/02/1944 | M | 0 | A | 46,XY[20] | NEGATIVE | NEGATIVE | NEGATIVE | NEGATIVE | NEGATIVE | NEGATIVE | | NEGATIVE | IGHV3-48*01 | IGHD2-2*01 | IGHJ6*02 | 100.00 |
| Patient 7 | 30/10/1953 | M | II | B | 46,XY,-17,+mar[5]/46,XY[20] | POSITIVE | NEGATIVE | NEGATIVE | NEGATIVE | POSITIVE | NEGATIVE | | POSITIVE | IGHV4-39*01 | IGHD3-3*01 | IGHJ5*02 | 100.00 |
| Patient 8 | 15/05/1955 | M | 0 | A | 46XY[25] | | | | | | NEGATIVE | | NEGATIVE | IGHV3-30*03 | IGHD6-6*01 | IGHJ6*02 | 100.00 |
| Patient 9 | 25/05/1967 | F | 0 | A | 45,X,add(X)(q?),del(1)(p?),add(8)(p?), add(9)(p?),add(12)(p?),-13,del(14)(q?), -17,add(19)(q?),+mar [4] | NEGATIVE | POSITIVE | NEGATIVE | NEGATIVE | POSITIVE | POSITIVE | | | | | | 100.00 |
| Patient 10 | 03/05/1952 | M | II | A | | POSITIVE | NEGATIVE | NEGATIVE | NEGATIVE | NEGATIVE | POSITIVE | A316T | NEGATIVE | IGHV2-26*01 | IGHD5-18*01 | IGHJ4*02 | 100.00 |
| Patient 11 | 30/10/1964 | M | II | A | 46,XY[20] | NEGATIVE | NEGATIVE | NEGATIVE | POSITIVE | NEGATIVE | NEGATIVE | | NEGATIVE | IGHV3-33*01 | IGHD3-9*01 | IGHJ4*02 | 100.00 |
| Patient 12 | 17/02/1932 | F | 0 | A | No metaphases | NEGATIVE | NEGATIVE | NEGATIVE | POSITIVE | POSITIVE | NEGATIVE | | | | | | 100.00 |
| Patient 13 | 8/5/1938 | M | I | A | 46, XY | POSITIVE | NEGATIVE | NEGATIVE | POSITIVE | NEGATIVE | | | | | | | |
| Patient 14 | 24/04/1961 | F | 0 | A | | NEGATIVE | NEGATIVE | NEGATIVE | NEGATIVE | NEGATIVE | NEGATIVE | | | | | | 100.00 |
| Patient 15 | 12/11/1946 | F | 0 | A | | POSITIVE | NEGATIVE | NEGATIVE | POSITIVE | NEGATIVE | NEGATIVE | | | | | | 98.00 |
| Patient 16 | 21/06/1971 | F | I | A | 46,XX[25] | NEGATIVE | POSITIVE | NEGATIVE | NEGATIVE | NEGATIVE | | | NEGATIVE | IGHV3-20*01 | IGHD3-22*01 | IGHJ3*02 | 94.10 |
| Patient 17 | 10/09/1965 | F | II | B | 46,XX[20] | | | NEGATIVE | NEGATIVE | NEGATIVE | NEGATIVE | | NEGATIVE | IGHV1-69*06 | IGHD3-16*02 | IGHJ1*01 | 99.30 |
| Patient 18 | 29/11/1960 | M | II | B | 46,XY,del(13)(q12q14)[2]/46,XY[18] | POSITIVE | NEGATIVE | NEGATIVE | NEGATIVE | NEGATIVE | NEGATIVE | | NEGATIVE | IGHV1-2*02 | IGHD6-19*01 | IGHJ4*02 | 100.00 |
| Patient 19 | 01/01/1941 | M | II | A | 46,XY[20] | POSITIVE | NEGATIVE | NEGATIVE | POSITIVE | NEGATIVE | NEGATIVE | | NEGATIVE | IGHV1-69*01 | IGHD6-19*01 | IGHJ5*02 | 100.00 |
| Patient 20 | 25/03/1940 | M | 0 | A | 46,XY,del(11)(q23)[16]/46,XY[4] | POSITIVE | NEGATIVE | NEGATIVE | POSITIVE | NEGATIVE | NEGATIVE | | NEGATIVE | IGHV3-11*01 | IGHD2-15*01 | IGHJ6*02 | 100.00 |
| Patient 21 | 05/07/1942 | M | I | A | 47,XY+12[12]/46,XY[3] | NEGATIVE | NEGATIVE | POSITIVE | NEGATIVE | NEGATIVE | NEGATIVE | | NEGATIVE | IGHV7-4-1*02 | IGHD6-19*01 | IGHJ4*02 | 100.00 |
| Patient 22 | 13/08/1943 | M | 0 | A | 46,XY[20] | NEGATIVE | NEGATIVE | NEGATIVE | NEGATIVE | NEGATIVE | POSITIVE | G818A | NEGATIVE | IGHV4-61*01 | IGHD3-3*01 | IGHJ5*02 | 100.00 |
| Patient 23 | 08/03/1935 | F | 0 | A | 46,XX[20] | NEGATIVE | NEGATIVE | NEGATIVE | NEGATIVE | NEGATIVE | NEGATIVE | | NEGATIVE | IGHV3-11*01 | IGHD3-10*01 | IGHJ6*02 | 100.00 |
| Patient 24 | 22/11/1942 | F | 0 | A | | POSITIVE | NEGATIVE | NEGATIVE | NEGATIVE | POSITIVE | NEGATIVE | | | | | | 98.64 |
| Patient 25 | 12/02/1938 | M | II | B | 47,XY,+12[11]/46,XY[14] | NEGATIVE | NEGATIVE | | | NEGATIVE | POSITIVE | G524C | NEGATIVE | IGHV1-69*09 | IGHD3-22*01 | IGHJ5*01 | 99.70 |
| Patient 26 | 24/10/1951 | M | IV | C | 46,XY[20] | POSITIVE | NEGATIVE | NEGATIVE | NEGATIVE | NEGATIVE | NEGATIVE | | NEGATIVE | IGHV1-69*01 | IGHD2-2*02 | IGHJ6*02 | 100.00 |
| Patient 27 | 11/04/1952 | M | 0 | A | 46,XY,del(13)(q13q21)[5]/46,XY[18] | | | | | NEGATIVE | NEGATIVE | | NEGATIVE | IGHV1-69*01 | IGHD3-10*01 | IGHJ6*03 | 100.00 |
| Patient 28 | 01/01/1945 | F | 0 | A | 46,XX,del(11)(q23),add(12)(p13)[3]/46,sdl, +6,-8,add(17)(p13)[14]/46,XX[8] | NEGATIVE | NEGATIVE | | POSITIVE | NEGATIVE | | | NEGATIVE | IGHV1-2*02 | IGHD5-5*01 | IGHJ4*02 | 100.00 |

* Patients who were included in the immune synapse bioassays are denoted in red font

| **SUPPLEMENTAL TABLE 2** |
|---|
| #start_read |
| start_read=0 |
| #end_read |
| end_read=5000000 |
| #type of cell, TCR=1, BCR=2 |
| cell_type=1 |
| # minimum length of initial sequence (unpaired read) |
| min_sequence_length=150 |
| #nucleotides with lower quality are considered bad |
| quality_limit=14 |
| #accepted sequence mean quality equal or higher of selected value |
| mean_quality=20 |
| # percentage of nts that can have low_quality |
| percentage_low_quality=0.15 |
| # minimum percentage of acceptable unidentified nucleotides (N) |
| percentage_Ns=0.01 |
| #minimum overlap length of paired reads |
| minimum_overlap_length=20 |
| #bestmatch_bestlen_ratio=0.2 |
| mismatch_ratio=0.25 |
| #continuousmatch |
| continuousmatch_thres=20 |
| #joined_quality_mean |
| joined_quality_mean=25 |
| #final_min_length of the final stitched sequence |
| joined_min_length=200 |
| #percentage of nts that can have low_quality in joined sequence |
| joined_perc_low_quality=0.07 |
| #nucleotides with lower quality are considered bad in joined sequence |
| joined_quality_limit=20 |
| #length to look for, before CDR3-end anchor |
| estimated_CDR3_length=75 |
| #nucleotides with lower quality are considered bad in selected length ahead of the CDR3 anchor |
| joined_CDR3_quality_limit=30 |
| #percentage_lowq_before_cdr3_anchor |
| percentage_lowq_before_cdr3_anchor=0.005 |

## SUPPLEMENTAL TABLE 4. Shared major T cell clonotypes across CLL patients

| AA Junction | Pt1 | Pt2 | Pt6 | Pt7 | Pt8 | Pt9 | Pt10 | Pt11 | Pt13 | Pt14 | Pt15 | Pt16 | Pt17 | Pt18 | Pt19 | Pt20 | Pt21 | Pt22 | Pt23 | Pt24 | Pt25 | Pt27 | Pt28 | Pt32 | Pt33 | Pt35 | Pt36 | Pt40 | Pt41 | Pt43 | Pt45 |
|---|---|---|---|---|---|---|---|---|---|---|---|---|---|---|---|---|---|---|---|---|---|---|---|---|---|---|---|---|---|---|---|
| CASSEESTLLNYGYTF | | | | | | | | | | | | 5.10 | | | | | 30.87 | | | | | | | | | | | | | | |
| CAISEKGGRDYGYTF | | | | | | | | | | | | | | | | | | 6.10 | | | | | | 5.14 | | | | | | | |
| CASSFGGTGNQPQHF | | | | | | | | | | | | | 6.40 | | | | | | | | | | | | | | 5.04 | | | | |
| CASSPPWTGELFF | | | | | | | | | | | | | | | | | | | | | | 8.14 | | | 5.06 | | | | | | |
| CASARGGNQPQHF | | | | | | | 5.03 | | | | 7.33 | | | | | | | | | | | | | | | | | | | | |
| CASSQDQGNNQPQHF | | | | | | | | | | | 12.03 | | | | | | | | | | | | | | | | | | | | 5.09 |
| CASSIDSPPSEKLFF | | | | | | | | | | | | | | 9.82 | | | | | | | | | | | | 5.20 | | | | |
| CASSESGGNQPQHF | | | | | | | | | | | | | 5.08 | | | | | 9.33 | | | | | | | | | | | 5.05 | |
| CASSLGPGANVLTF | | | 5.08 | | 13.89 | | | | | | | | | | | | | | | | | | | | | | | | | | |
| CASSPGTGYTF | | | | | | | | | | | | | | | 12.95 | 5.09 | | | | | | | | | | | | | | | |
| CASSSANYGYTF | | | | 18.44 | | | | | | | | 5.08 | 15.95 | 7.27 | 6.89 | | | | 10.75 | | | | | | | 5.11 | | | | |
| CASSSDSKIGELFF | | | | | | | | | | | | | | 24.14 | 5.08 | | | | | | | | | | | | | | | |
| CASSIFGELFF | | 15.03 | 8.88 | | | | | | | | | | | | | | | | | | | | | | | | | | | | |
| CASSTTGGDGYTF | | | | | | | | | | | 8.53 | | | | 5.07 | | | | | | | 5.26 | | | | | | | | | |
| CASTPGDTIYF | | | | | | | | | 5.05 | | | | | | | 5.95 | | | | | | | | | | | | | | | |
| CSVDPSGTGGEGYTF | | | 17.57 | | | | | 5.09 | | | | | 5.06 | 5.03 | | | | | | | | | | | | | | | | | |
| CSVGSGAGGQSNYGYTF | | | | | 13.98 | | | | | | | | | 5.05 | | | | | | | | | | | | | | | | | |
| CSVGSGGTNEKLFF | | | 13.20 | | | | | | | | | | | | | | | 5.04 | 5.69 | | | | | | | | | | | | |
| CSVGTGGTNEKLFF | | 5.16 | | | | | | | | | | | | | | | 6.48 | 5.03 | | | 5.23 | | | | | 5.07 | | | 5.88 | | |
| CSVLPRQGREDGYTF | | | | | | | | | | | | | | | | 5.09 | | 23.19 | | | | | | | | | | | | | |
| CASSPSRNTEAFF | | | | | | | | | | | | | | | | 6.83 | | | | | | | 5.91 | | | | | | | | |
| CASSLEGDRPQHF | | | | | | 6.00 | | | | 6.02 | | | | | | | | | 5.09 | | | | | | | | | | | | |
| CASSWDKSYGYTF | | | | | | | | | | | | | | | 6.63 | | | | | | | | 5.09 | | | | | | | | |
| CASSGTNANYGYTF | | | 17.12 | | | | | 5.09 | | | | | | | | | | | | | | | | | | | | | | | |
| CASSFGRGYEKLFF | | | | | | | | | | | | | 6.40 | | | 5.27 | | 5.02 | | 6.11 | | | | | | | | | | | |
| CASSPSTGTIYGYTF | | | | 5.39 | | 5.48 | | | | | | | 5.99 | | | | | | | | | | | | | | | | | | |
| CASSPVTGTGSYGYTF | | | | | | | | | | | | | 5.19 | 21.44 | | | | | | | | | | | | | 5.08 | | | | |
| CASSYGDSYGYTF | 5.65 | | | | | | | | | | | 5.13 | | | | | | | | | | | | | | | | | | | |
| CASSYQTGAAYGYTF | | 9.50 | | | | | | | | | | 11.84 | | | | | | | | | | | | | | | | | | | |
| CASSLAPGTTNEKLFF | | | | | | 5.21 | | | | | | | | | | | | 11.10 | | | | | | | | | | | | | |

**% frequency color scale**

**5%** → **32%**

* For across-patient comparisons, the concatenated sum of unique clonotypes from all PB samples of the same patient was considered. For each clonotype, the highest frequency among one patient's samples is reported here.

**Suppl. Fig. 1. Flow cytometry gating strategy.**

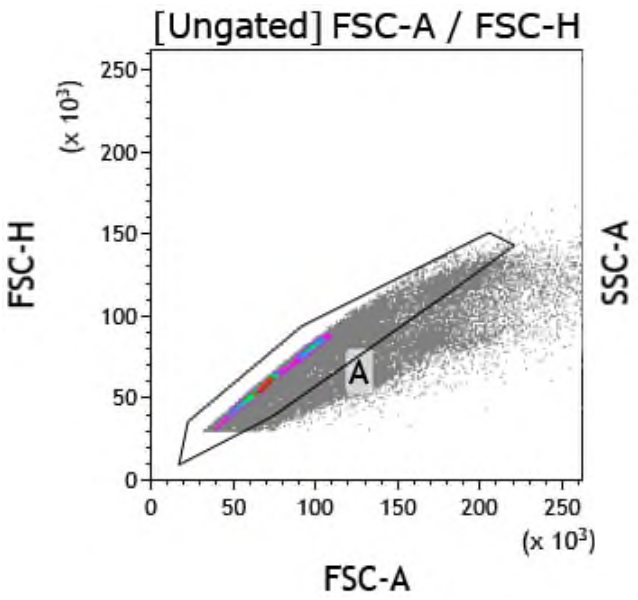


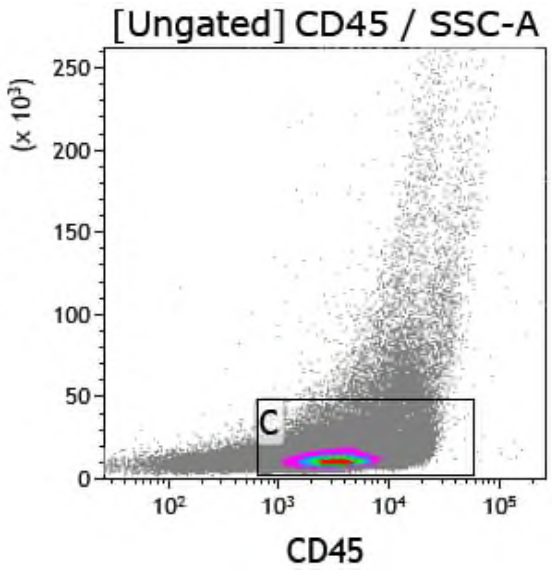


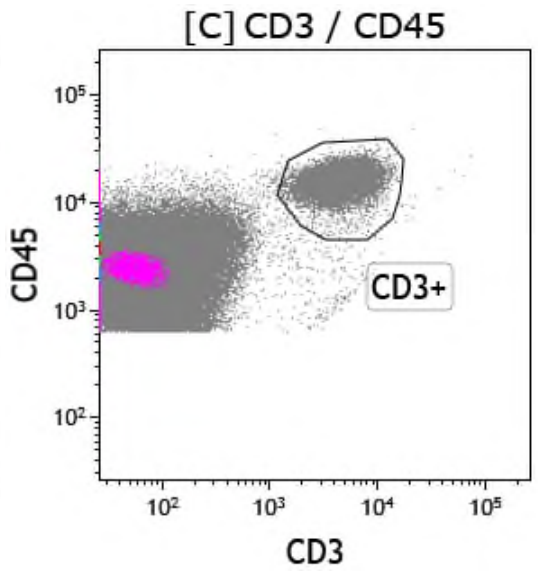


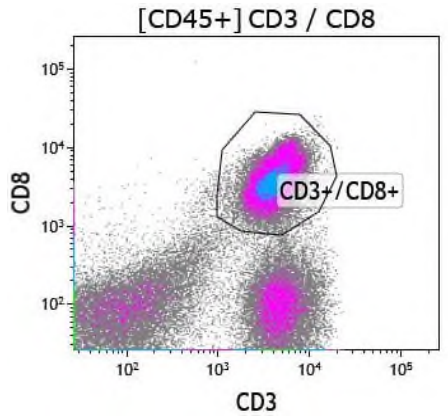


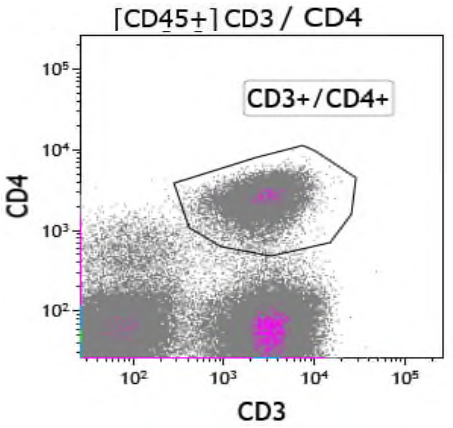


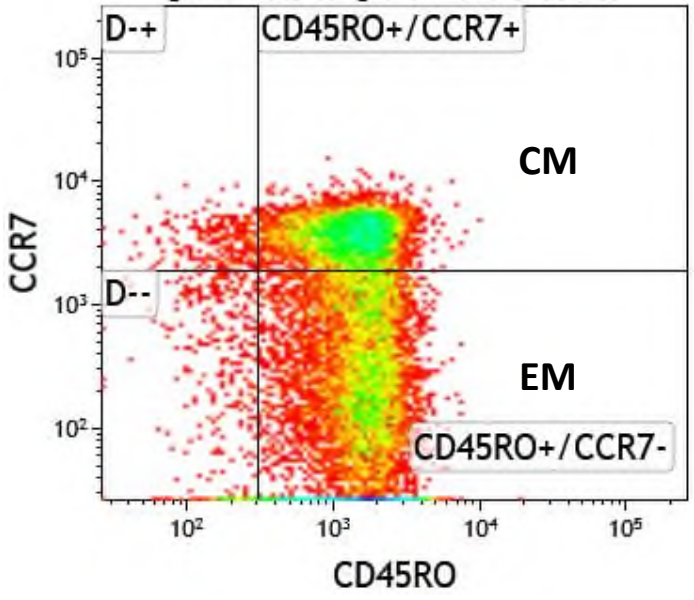


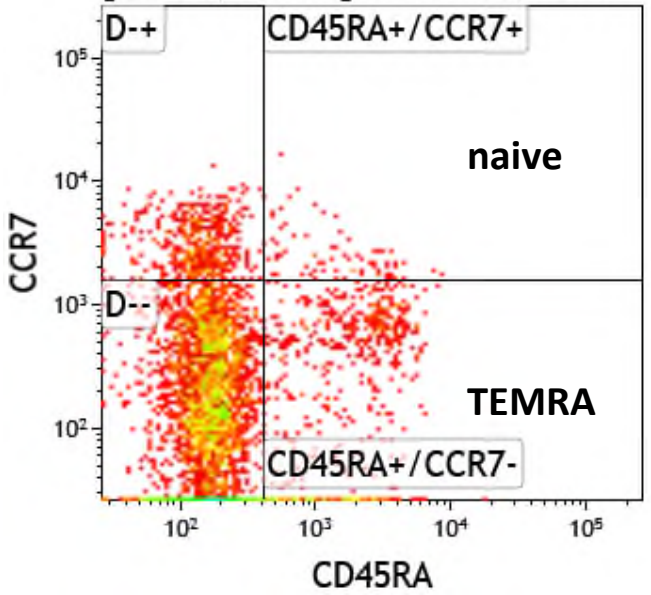

A

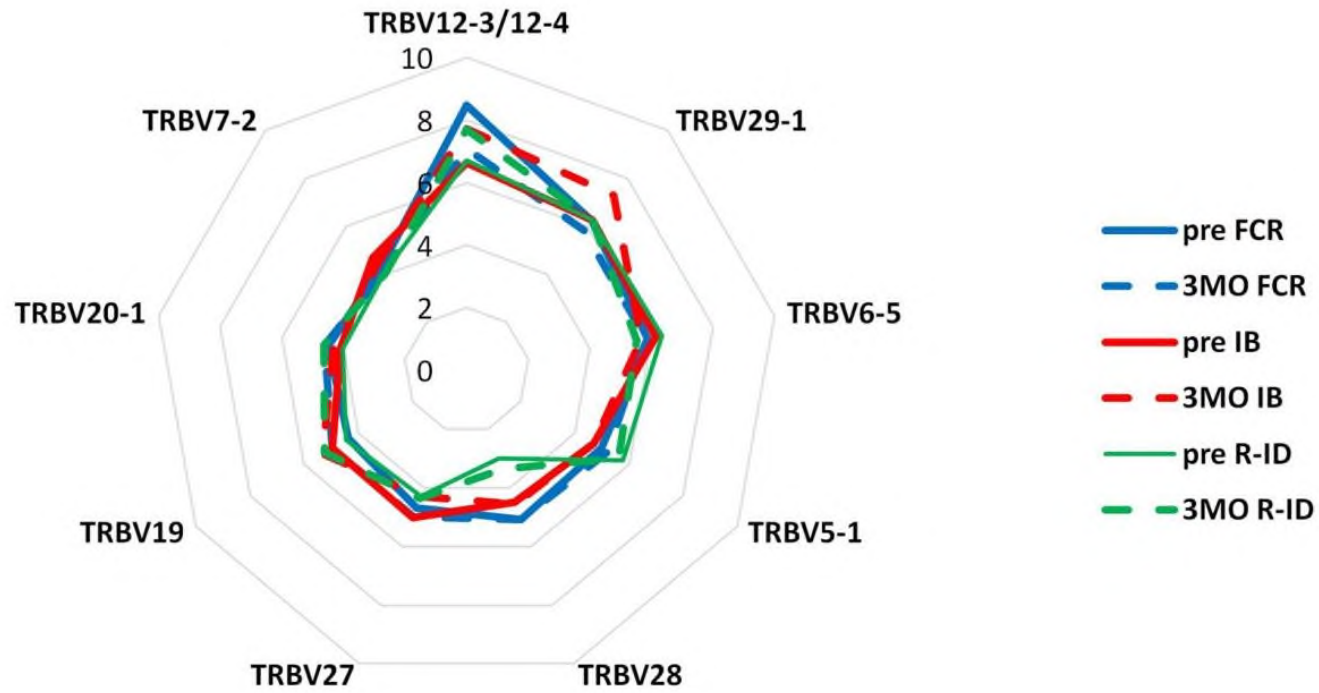


B

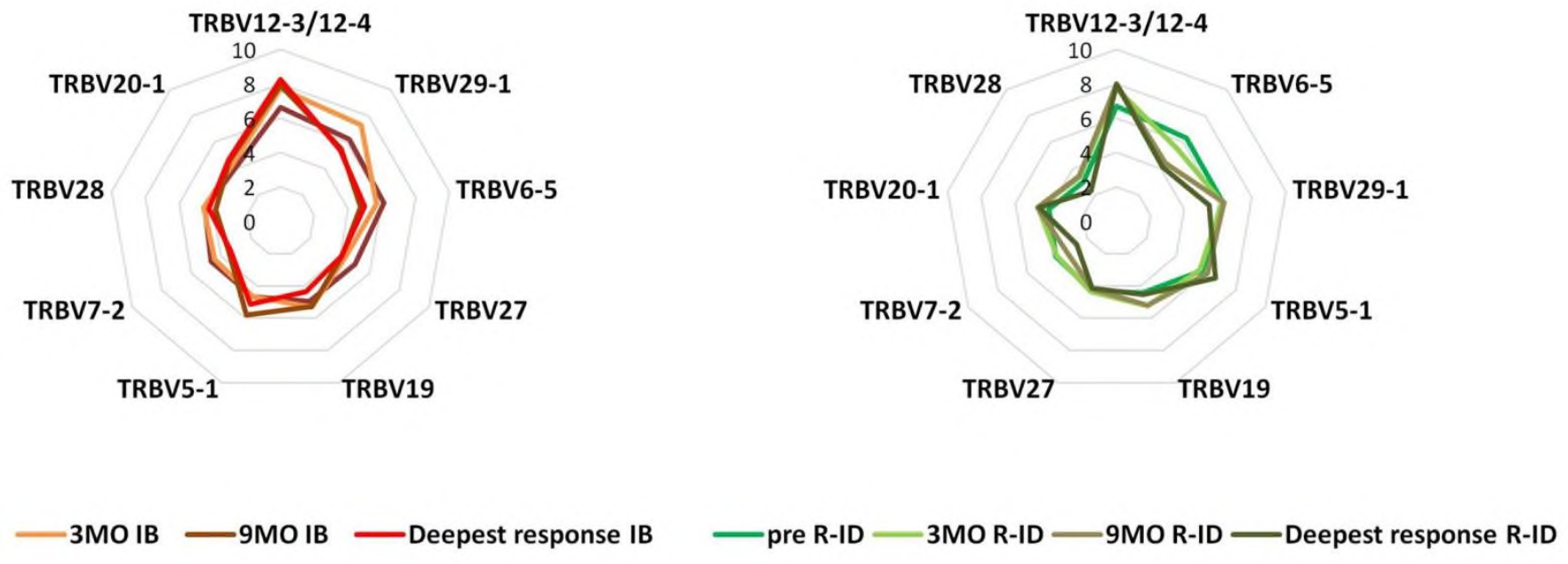


**Suppl. Fig. 2. A. The TRBV gene repertoire remains stable at the 3-month timepoint in all treatment groups.** The % frequency of the 9 most frequent TRBV genes pre-tretament and at the 3-month timepoint per treatment group is depicted. **B. The TRBV gene repertoire remains stable over time for the IB and R-ID groups.** The % frequency of the 9 most frequent TRBV genes pre-treatment, at 3 months, 9 months and deepest clinical response is depicted for the IB and R-ID group.

**Suppl. Fig. 3A**

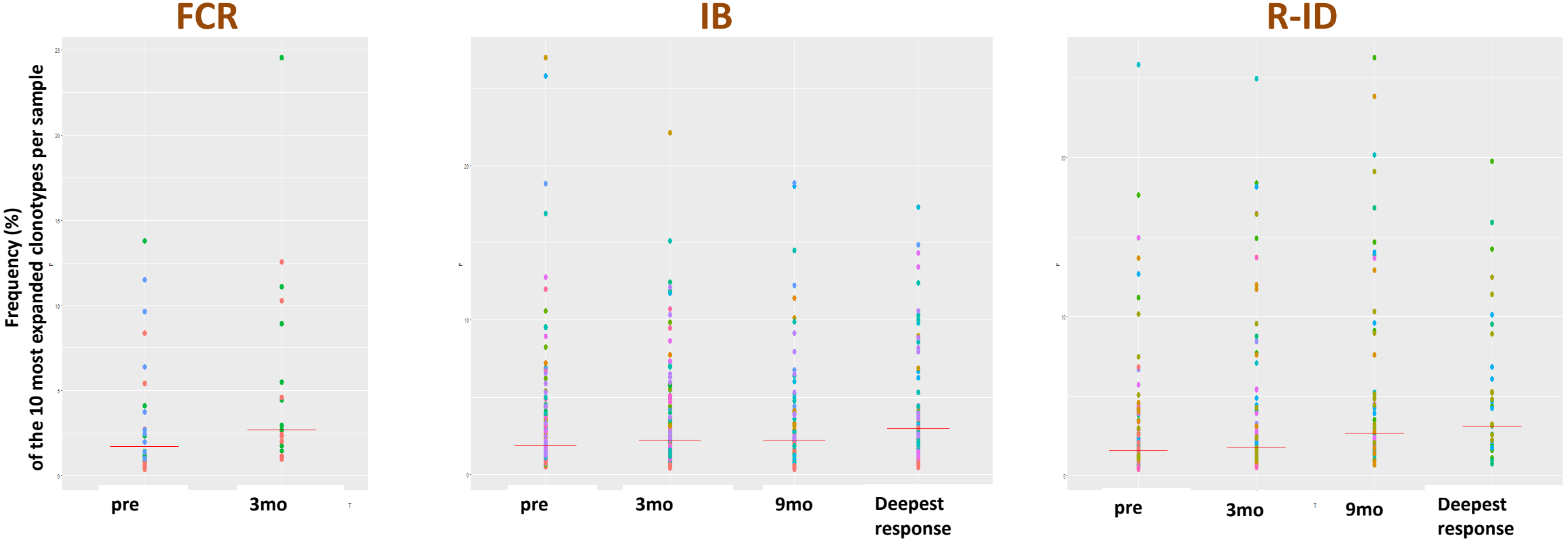
FCR
IB
R-ID
Frequency (%)
of the 10 most expanded clonotypes per sample
pre
3mo
9mo
Deepest response

**Suppl. Fig. 3B**

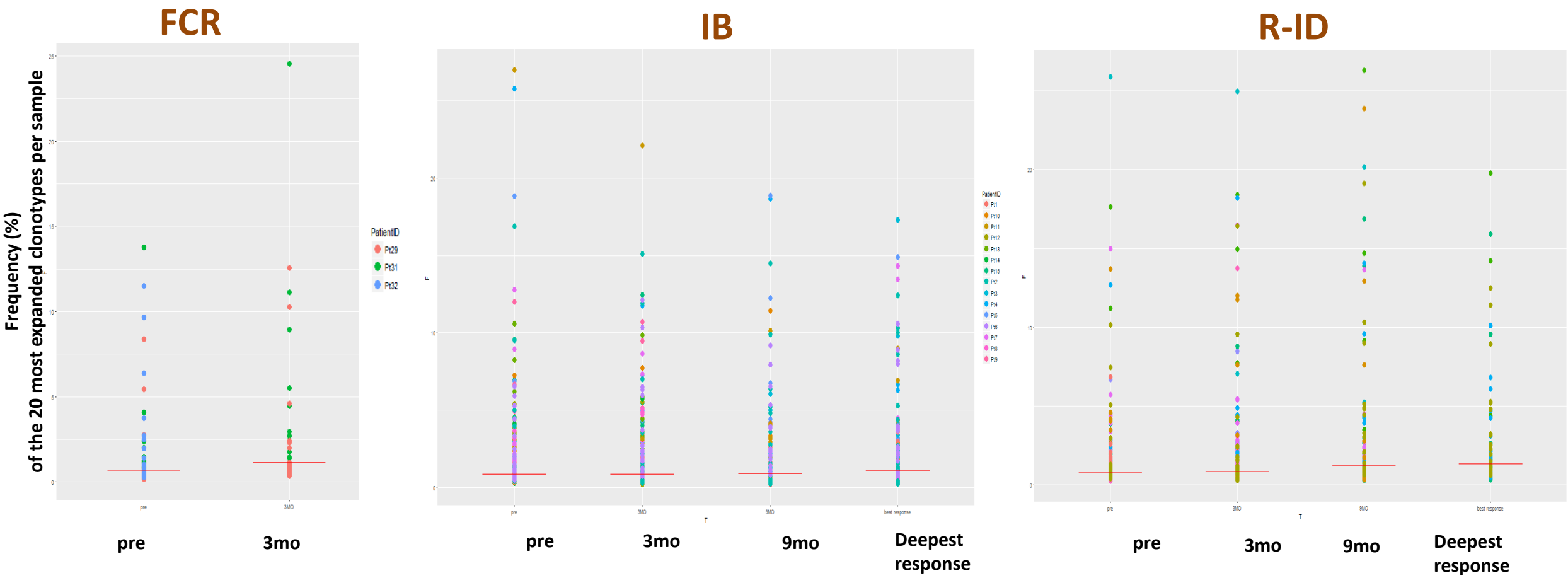
FCR
IB
R-ID
Frequency (%) of the 20 most expanded clonotypes per sample
PatientID
Pt29
Pt31
Pt32
pre
3MO
9MO
best response
T
pre
3mo
pre
3mo
9mo
Deepest response
pre
3mo
9mo
Deepest response

**Suppl. Fig. 3C**

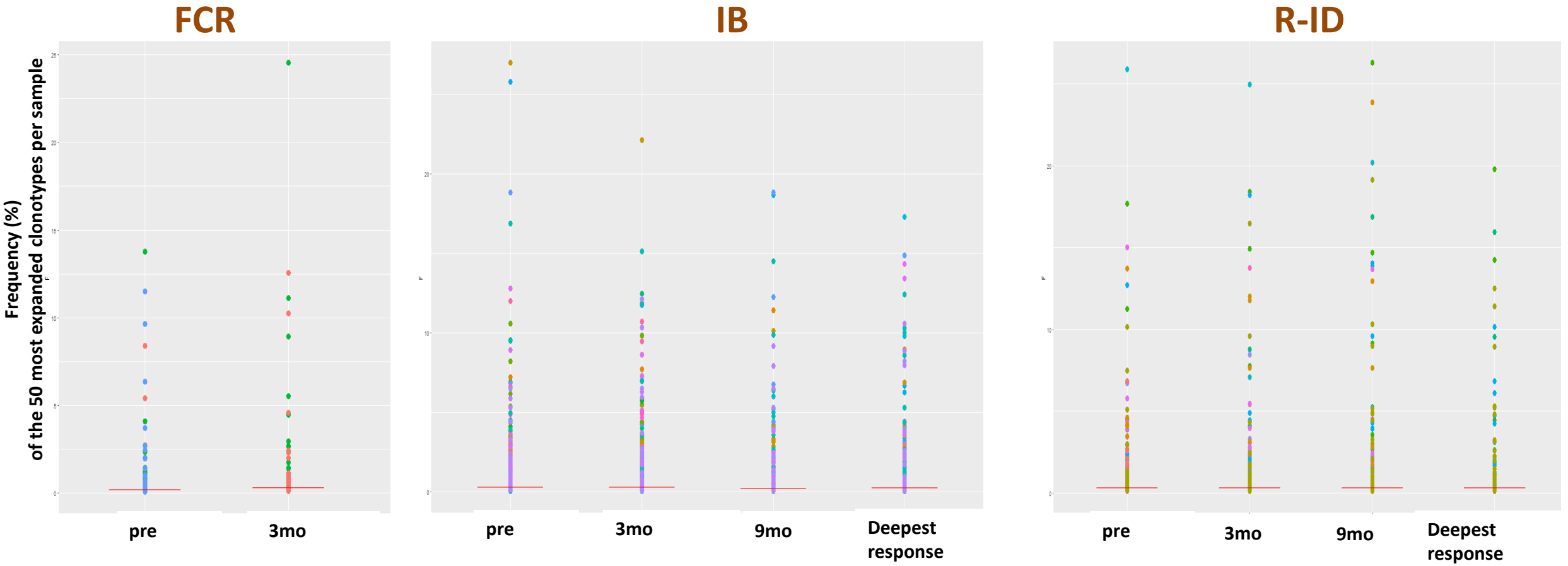
FCR
IB
R-ID
Frequency (%) of the 50 most expanded clonotypes per sample
pre
3mo
pre
3mo
9mo
Deepest response
pre
3mo
9mo
Deepest response

**Suppl. Fig. 3D**

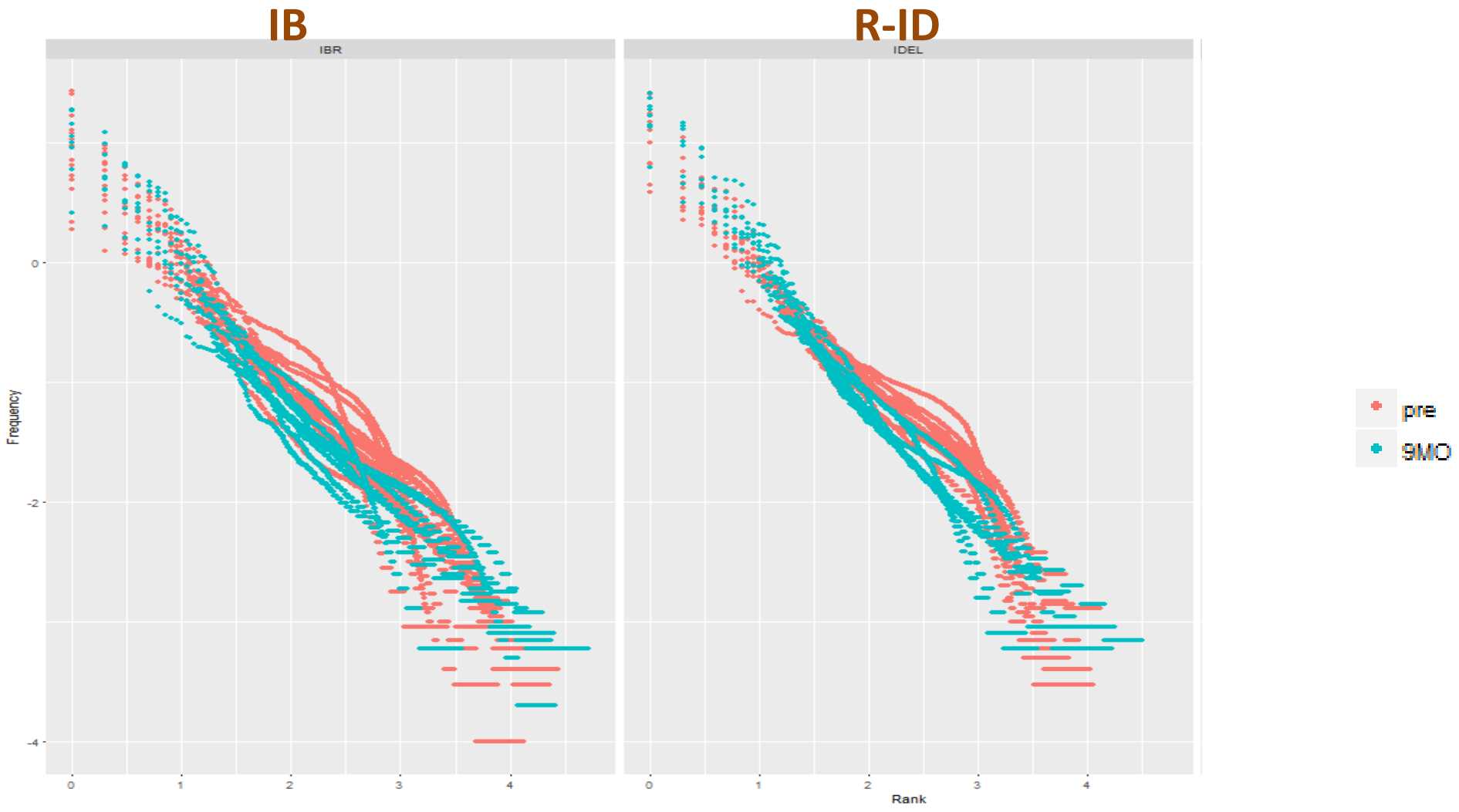


Increase of clonality post-treatment results from the expansion of the major clonotypes. A, B, C: Frequency (%) of the 10, 20 and 50 most expanded clonotypes (dots) per sample overtime, respectively. Clonotypes of the same patient are represented by the same color. The vertical line represents the median value. D: Clonotype frequency against rank plot for the IB and R-ID pre- and +9mo post-treatment.

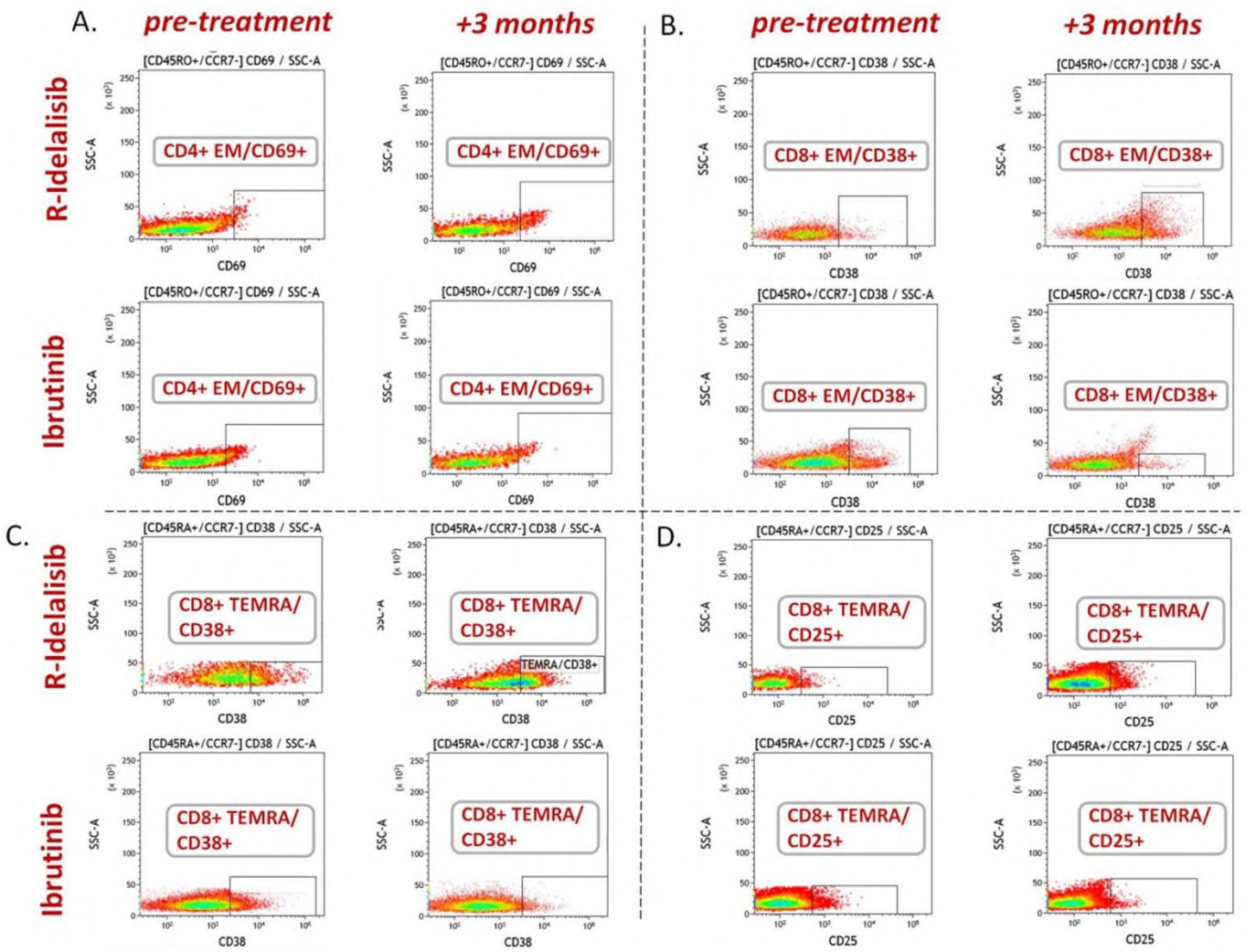


**Suppl. Fig. 4. R-ID increases the expression of activation markers on effector memory T cells as compared to IB treatment.** Each panel (A, B, C, D) shows how treatment affects the expression of an activation marker on a specific T-cell subpopulation for a pair of an R-ID and an IB-treated patient. (A: CD69 expression on $CD4^+$ EM T cells; B: CD38 expression on $CD8^+$ EM T cells; C: CD38 expression on $CD8^+$ TEMRA cells; and, D: CD25 expression on $CD8^+$ TEMRA cells)

**SUPPLEMENTAL TABLE 1. Study cohort demographics and clinicobiological information**

| Patient ID | Date of birth | Sex | Rai at diagnosis | Binet at diagnosis | Karyotype | FISH del(13q) monoallelic result | FISH del(13q) biallelic result | FISH trisomy 12 result | FISH del(11q) result | FISH del(17p) result | TP53 abnormality | TP53 nucleotide change | NOTCH1 mutation result | IGHV | IGHD | IGHJ | IGHV GI Identity % |
|---|---|---|---|---|---|---|---|---|---|---|---|---|---|---|---|---|---|
| Patient 1 | 15/08/1966 | M | I | A | 46,XY[20] | NEGATIVE | NEGATIVE | NEGATIVE | NEGATIVE | NEGATIVE | NEGATIVE | | NEGATIVE | IGHV2-5*01 | IGHD3-3*02 | IGHJ4*02 | 100.00 |
| Patient 2 | 16/05/1952 | M | II | B | 46,XY, del(17)(p13)[3]/45, X,-Y[3]/46,XY[24] | | | | | POSITIVE | POSITIVE | A536G | NEGATIVE | IGHV5-51*01 | IGHD2-2*01 | IGHJ4*01 | 100.00 |
| Patient 3 | 01/01/1953 | F | II | B | 46,XX,t(14;22)(q34;q11)[6]/46XX[22] | NEGATIVE | NEGATIVE | NEGATIVE | NEGATIVE | POSITIVE | | | | IGHV3-48*02 | IGHD1-26*01 | IGHJ1*01 | 98.96 |
| Patient 4 | 22/07/1952 | M | I | A | | NEGATIVE | NEGATIVE | NEGATIVE | NEGATIVE | NEGATIVE | NEGATIVE | | NEGATIVE | IGHV1-69*04 | IGHD3-10*01 | IGHJ6*02 | 100.00 |
| Patient 5 | 24/04/1948 | F | IV | C | 46,XX[20] | POSITIVE | NEGATIVE | NEGATIVE | NEGATIVE | NEGATIVE | NEGATIVE | | NEGATIVE | IGHV3-30-3*01 | IGHD3-10*01 | IGHJ4*02 | 100.00 |
| Patient 6 | 05/02/1944 | M | 0 | A | 46,XY[20] | NEGATIVE | NEGATIVE | NEGATIVE | NEGATIVE | NEGATIVE | NEGATIVE | | NEGATIVE | IGHV3-48*01 | IGHD2-2*01 | IGHJ6*02 | 100.00 |
| Patient 7 | 30/10/1953 | M | II | B | 46,XY,-17,+mar[5]/46,XY[20] | POSITIVE | NEGATIVE | NEGATIVE | NEGATIVE | POSITIVE | NEGATIVE | | POSITIVE | IGHV4-39*01 | IGHD3-3*01 | IGHJ5*02 | 100.00 |
| Patient 8 | 15/05/1955 | M | 0 | A | 46XY[25] | | | | | | NEGATIVE | | NEGATIVE | IGHV3-30*03 | IGHD6-6*01 | IGHJ6*02 | 100.00 |
| Patient 9 | 25/05/1967 | F | 0 | A | 45,X,add(X)(q?),del(1)(p?),add(8)(p?), add(9)(p?),add(12)(p?),-13,del(14)(q?), -17,add(19)(q?),+mar [4] | NEGATIVE | POSITIVE | NEGATIVE | NEGATIVE | POSITIVE | POSITIVE | | | | | | 100.00 |
| Patient 10 | 03/05/1952 | M | II | A | | POSITIVE | NEGATIVE | NEGATIVE | NEGATIVE | NEGATIVE | POSITIVE | A316T | NEGATIVE | IGHV2-26*01 | IGHD5-18*01 | IGHJ4*02 | 100.00 |
| Patient 11 | 30/10/1964 | M | II | A | 46,XY[20] | NEGATIVE | NEGATIVE | NEGATIVE | POSITIVE | NEGATIVE | NEGATIVE | | NEGATIVE | IGHV3-33*01 | IGHD3-9*01 | IGHJ4*02 | 100.00 |
| Patient 12 | 17/02/1932 | F | 0 | A | No metaphases | NEGATIVE | NEGATIVE | NEGATIVE | POSITIVE | POSITIVE | NEGATIVE | | | | | | 100.00 |
| Patient 13 | 8/5/1938 | M | I | A | 46, XY | POSITIVE | NEGATIVE | NEGATIVE | POSITIVE | NEGATIVE | | | | | | | |
| Patient 14 | 24/04/1961 | F | 0 | A | | NEGATIVE | NEGATIVE | NEGATIVE | NEGATIVE | NEGATIVE | NEGATIVE | | | | | | 100.00 |
| Patient 15 | 12/11/1946 | F | 0 | A | | POSITIVE | NEGATIVE | NEGATIVE | POSITIVE | NEGATIVE | NEGATIVE | | | | | | 98.00 |
| Patient 16 | 21/06/1971 | F | I | A | 46,XX[25] | NEGATIVE | POSITIVE | NEGATIVE | NEGATIVE | NEGATIVE | | | NEGATIVE | IGHV3-20*01 | IGHD3-22*01 | IGHJ3*02 | 94.10 |
| Patient 17 | 10/09/1965 | F | II | B | 46,XX[20] | | | NEGATIVE | NEGATIVE | NEGATIVE | NEGATIVE | | NEGATIVE | IGHV1-69*06 | IGHD3-16*02 | IGHJ1*01 | 99.30 |
| Patient 18 | 29/11/1960 | M | II | B | 46,XY,del(13)(q12q14)[2]/46,XY[18] | POSITIVE | NEGATIVE | NEGATIVE | NEGATIVE | NEGATIVE | NEGATIVE | | NEGATIVE | IGHV1-2*02 | IGHD6-19*01 | IGHJ4*02 | 100.00 |
| Patient 19 | 01/01/1941 | M | II | A | 46,XY[20] | POSITIVE | NEGATIVE | NEGATIVE | POSITIVE | NEGATIVE | NEGATIVE | | NEGATIVE | IGHV1-69*01 | IGHD6-19*01 | IGHJ5*02 | 100.00 |
| Patient 20 | 25/03/1940 | M | 0 | A | 46,XY,del(11)(q23)[16]/46,XY[4] | POSITIVE | NEGATIVE | NEGATIVE | POSITIVE | NEGATIVE | NEGATIVE | | NEGATIVE | IGHV3-11*01 | IGHD2-15*01 | IGHJ6*02 | 100.00 |
| Patient 21 | 05/07/1942 | M | I | A | 47,XY+12[12]/46,XY[3] | NEGATIVE | NEGATIVE | POSITIVE | NEGATIVE | NEGATIVE | NEGATIVE | | NEGATIVE | IGHV7-4-1*02 | IGHD6-19*01 | IGHJ4*02 | 100.00 |
| Patient 22 | 13/08/1943 | M | 0 | A | 46,XY[20] | NEGATIVE | NEGATIVE | NEGATIVE | NEGATIVE | NEGATIVE | POSITIVE | G818A | NEGATIVE | IGHV4-61*01 | IGHD3-3*01 | IGHJ5*02 | 100.00 |
| Patient 23 | 08/03/1935 | F | 0 | A | 46,XX[20] | NEGATIVE | NEGATIVE | NEGATIVE | NEGATIVE | NEGATIVE | NEGATIVE | | NEGATIVE | IGHV3-11*01 | IGHD3-10*01 | IGHJ6*02 | 100.00 |
| Patient 24 | 22/11/1942 | F | 0 | A | | POSITIVE | NEGATIVE | NEGATIVE | NEGATIVE | POSITIVE | NEGATIVE | | | | | | 98.64 |
| Patient 25 | 12/02/1938 | M | II | B | 47,XY,+12[11]/46,XY[14] | NEGATIVE | NEGATIVE | | | NEGATIVE | POSITIVE | G524C | NEGATIVE | IGHV1-69*09 | IGHD3-22*01 | IGHJ5*01 | 99.70 |
| Patient 26 | 24/10/1951 | M | IV | C | 46,XY[20] | POSITIVE | NEGATIVE | NEGATIVE | NEGATIVE | NEGATIVE | NEGATIVE | | NEGATIVE | IGHV1-69*01 | IGHD2-2*02 | IGHJ6*02 | 100.00 |
| Patient 27 | 11/04/1952 | M | 0 | A | 46,XY,del(13)(q13q21)[5]/46,XY[18] | | | | | NEGATIVE | NEGATIVE | | NEGATIVE | IGHV1-69*01 | IGHD3-10*01 | IGHJ6*03 | 100.00 |
| Patient 28 | 01/01/1945 | F | 0 | A | 46,XX,del(11)(q23),add(12)(p13)[3]/46,sdl, +6,-8,add(17)(p13)[14]/46,XX[8] | NEGATIVE | NEGATIVE | | POSITIVE | NEGATIVE | | | NEGATIVE | IGHV1-2*02 | IGHD5-5*01 | IGHJ4*02 | 100.00 |

* Patients who were included in the immune synapse bioassays are denoted in red font

| **SUPPLEMENTAL TABLE 2** |
|---|
| #start_read |
| start_read=0 |
| #end_read |
| end_read=5000000 |
| #type of cell, TCR=1, BCR=2 |
| cell_type=1 |
| # minimum length of initial sequence (unpaired read) |
| min_sequence_length=150 |
| #nucleotides with lower quality are considered bad |
| quality_limit=14 |
| #accepted sequence mean quality equal or higher of selected value |
| mean_quality=20 |
| # percentage of nts that can have low_quality |
| percentage_low_quality=0.15 |
| # minimum percentage of acceptable unidentified nucleotides (N) |
| percentage_Ns=0.01 |
| #minimum overlap length of paired reads |
| minimum_overlap_length=20 |
| #bestmatch_bestlen_ratio=0.2 |
| mismatch_ratio=0.25 |
| #continuousmatch |
| continuousmatch_thres=20 |
| #joined_quality_mean |
| joined_quality_mean=25 |
| #final_min_length of the final stitched sequence |
| joined_min_length=200 |
| #percentage of nts that can have low_quality in joined sequence |
| joined_perc_low_quality=0.07 |
| #nucleotides with lower quality are considered bad in joined sequence |
| joined_quality_limit=20 |
| #length to look for, before CDR3-end anchor |
| estimated_CDR3_length=75 |
| #nucleotides with lower quality are considered bad in selected length ahead of the CDR3 anchor |
| joined_CDR3_quality_limit=30 |
| #percentage_lowq_before_cdr3_anchor |
| percentage_lowq_before_cdr3_anchor=0.005 |

## SUPPLEMENTAL TABLE 4. Shared major T cell clonotypes across CLL patients

| AA Junction | Pt1 | Pt2 | Pt6 | Pt7 | Pt8 | Pt9 | Pt10 | Pt11 | Pt13 | Pt14 | Pt15 | Pt16 | Pt17 | Pt18 | Pt19 | Pt20 | Pt21 | Pt22 | Pt23 | Pt24 | Pt25 | Pt27 | Pt28 | Pt32 | Pt33 | Pt35 | Pt36 | Pt40 | Pt41 | Pt43 | Pt45 |
|---|---|---|---|---|---|---|---|---|---|---|---|---|---|---|---|---|---|---|---|---|---|---|---|---|---|---|---|---|---|---|---|
| CASSEESTLLNYGYTF | | | | | | | | | | | | 5.10 | | | | | 30.87 | | | | | | | | | | | | | | |
| CAISEKGGRDYGYTF | | | | | | | | | | | | | | | | | | 6.10 | | | | | | 5.14 | | | | | | | |
| CASSFGGTGNQPQHF | | | | | | | | | | | | | 6.40 | | | | | | | | | | | | | | 5.04 | | | | |
| CASSPPWTGELFF | | | | | | | | | | | | | | | | | | | | | | 8.14 | | | 5.06 | | | | | | |
| CASARGGNQPQHF | | | | | | | 5.03 | | | | 7.33 | | | | | | | | | | | | | | | | | | | | |
| CASSQDQGNNQPQHF | | | | | | | | | | | 12.03 | | | | | | | | | | | | | | | | | | | | 5.09 |
| CASSIDSPPSEKLFF | | | | | | | | | | | | | | 9.82 | | | | | | | | | | | | 5.20 | | | | |
| CASSESGGNQPQHF | | | | | | | | | | | | | 5.08 | | | | | 9.33 | | | | | | | | | | | 5.05 | |
| CASSLGPGANVLTF | | | 5.08 | | 13.89 | | | | | | | | | | | | | | | | | | | | | | | | | | |
| CASSPGTGYTF | | | | | | | | | | | | | | | 12.95 | 5.09 | | | | | | | | | | | | | | | |
| CASSSANYGYTF | | | | 18.44 | | | | | | | | 5.08 | 15.95 | 7.27 | 6.89 | | | | 10.75 | | | | | | | 5.11 | | | | |
| CASSSDSKIGELFF | | | | | | | | | | | | | | 24.14 | 5.08 | | | | | | | | | | | | | | | |
| CASSIFGELFF | | 15.03 | 8.88 | | | | | | | | | | | | | | | | | | | | | | | | | | | | |
| CASSTTGGDGYTF | | | | | | | | | | | 8.53 | | | | 5.07 | | | | | | | 5.26 | | | | | | | | | |
| CASTPGDTIYF | | | | | | | | | 5.05 | | | | | | | 5.95 | | | | | | | | | | | | | | | |
| CSVDPSGTGGEGYTF | | | 17.57 | | | | | 5.09 | | | | | 5.06 | 5.03 | | | | | | | | | | | | | | | | | |
| CSVGSGAGGQSNYGYTF | | | | | 13.98 | | | | | | | | | 5.05 | | | | | | | | | | | | | | | | | |
| CSVGSGGTNEKLFF | | | 13.20 | | | | | | | | | | | | | | | 5.04 | 5.69 | | | | | | | | | | | | |
| CSVGTGGTNEKLFF | | 5.16 | | | | | | | | | | | | | | | 6.48 | 5.03 | | | 5.23 | | | | | 5.07 | | | 5.88 | | |
| CSVLPRQGREDGYTF | | | | | | | | | | | | | | | | 5.09 | | 23.19 | | | | | | | | | | | | | |
| CASSPSRNTEAFF | | | | | | | | | | | | | | | | 6.83 | | | | | | | 5.91 | | | | | | | | |
| CASSLEGDRPQHF | | | | | | 6.00 | | | | 6.02 | | | | | | | | | 5.09 | | | | | | | | | | | | |
| CASSWDKSYGYTF | | | | | | | | | | | | | | | 6.63 | | | | | | | | 5.09 | | | | | | | | |
| CASSGTNANYGYTF | | | 17.12 | | | | | 5.09 | | | | | | | | | | | | | | | | | | | | | | | |
| CASSFGRGYEKLFF | | | | | | | | | | | | | 6.40 | | | 5.27 | | 5.02 | | 6.11 | | | | | | | | | | | |
| CASSPSTGTIYGYTF | | | | 5.39 | | 5.48 | | | | | | | 5.99 | | | | | | | | | | | | | | | | | | |
| CASSPVTGTGSYGYTF | | | | | | | | | | | | | 5.19 | 21.44 | | | | | | | | | | | | | 5.08 | | | | |
| CASSYGDSYGYTF | 5.65 | | | | | | | | | | | 5.13 | | | | | | | | | | | | | | | | | | | |
| CASSYQTGAAYGYTF | | 9.50 | | | | | | | | | | 11.84 | | | | | | | | | | | | | | | | | | | |
| CASSLAPGTTNEKLFF | | | | | | 5.21 | | | | | | | | | | | | 11.10 | | | | | | | | | | | | | |

**% frequency color scale**

**5%** → **32%**

* For across-patient comparisons, the concatenated sum of unique clonotypes from all PB samples of the same patient was considered. For each clonotype, the highest frequency among one patient's samples is reported here.

**Suppl. Fig. 1. Flow cytometry gating strategy.**

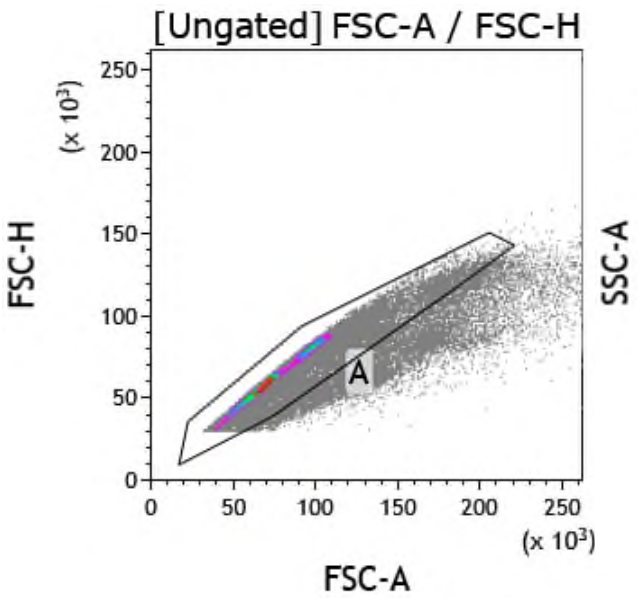


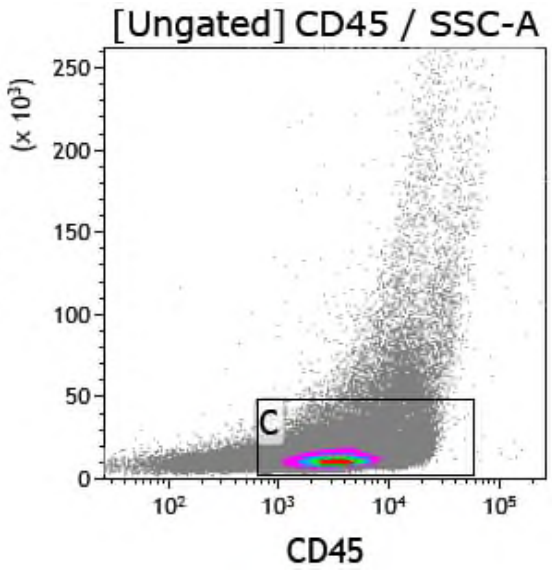


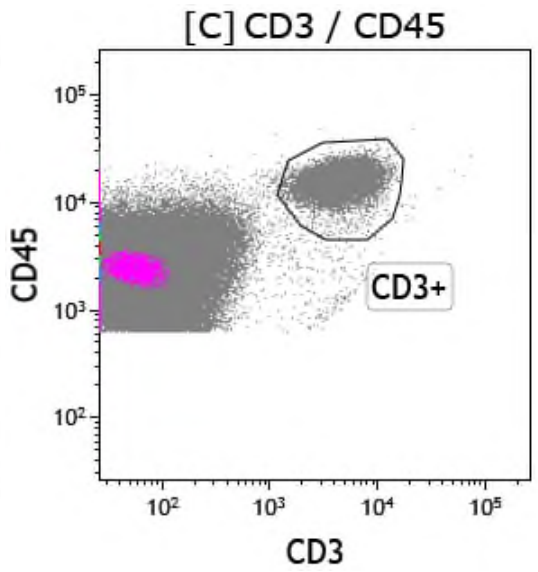


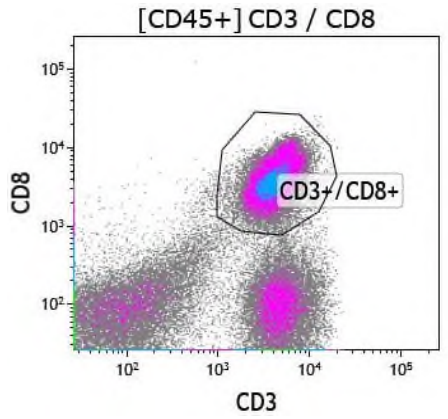


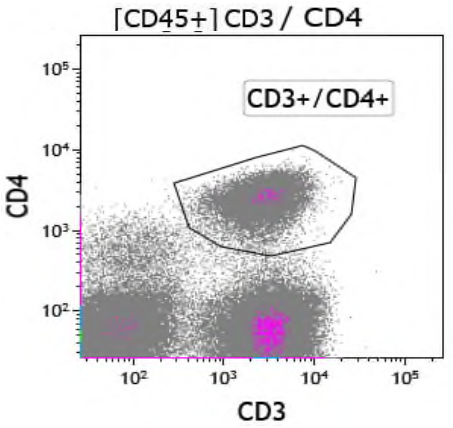


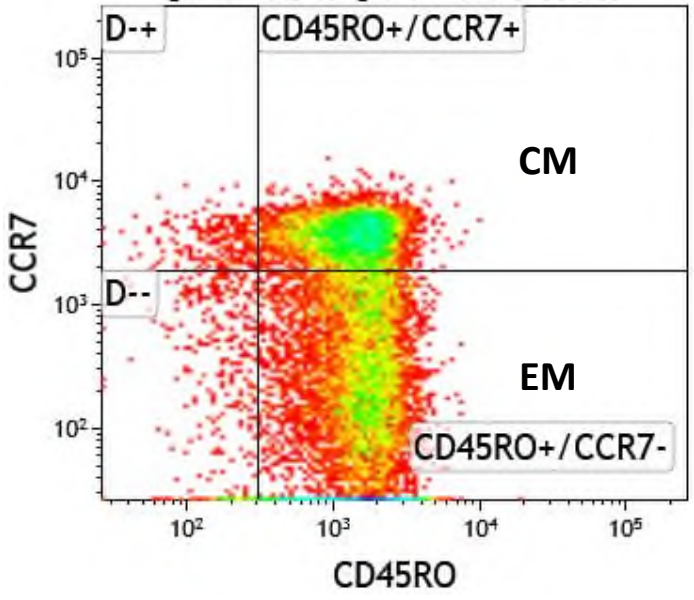


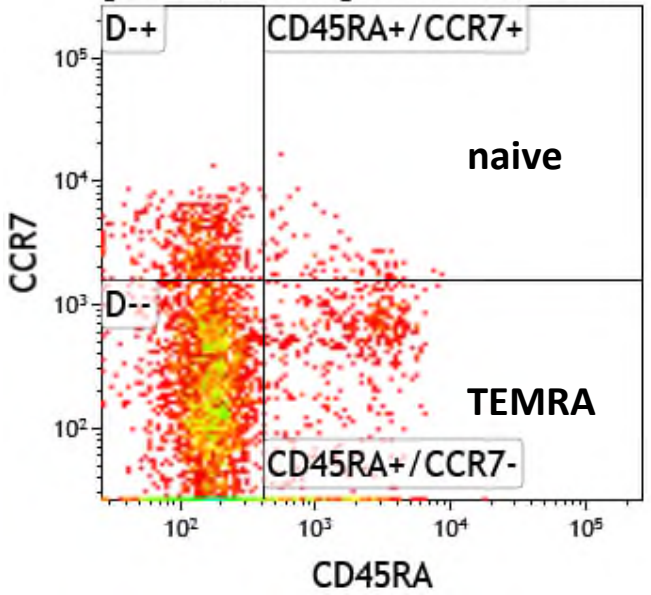

A

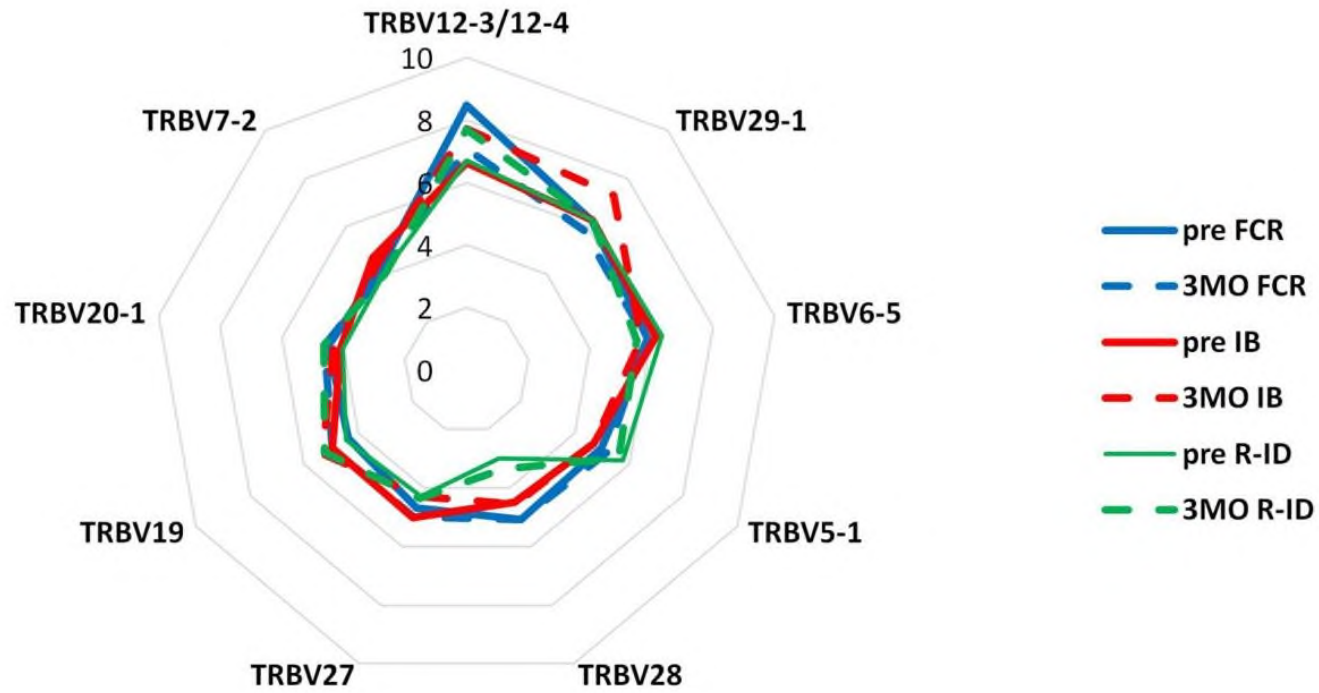


B

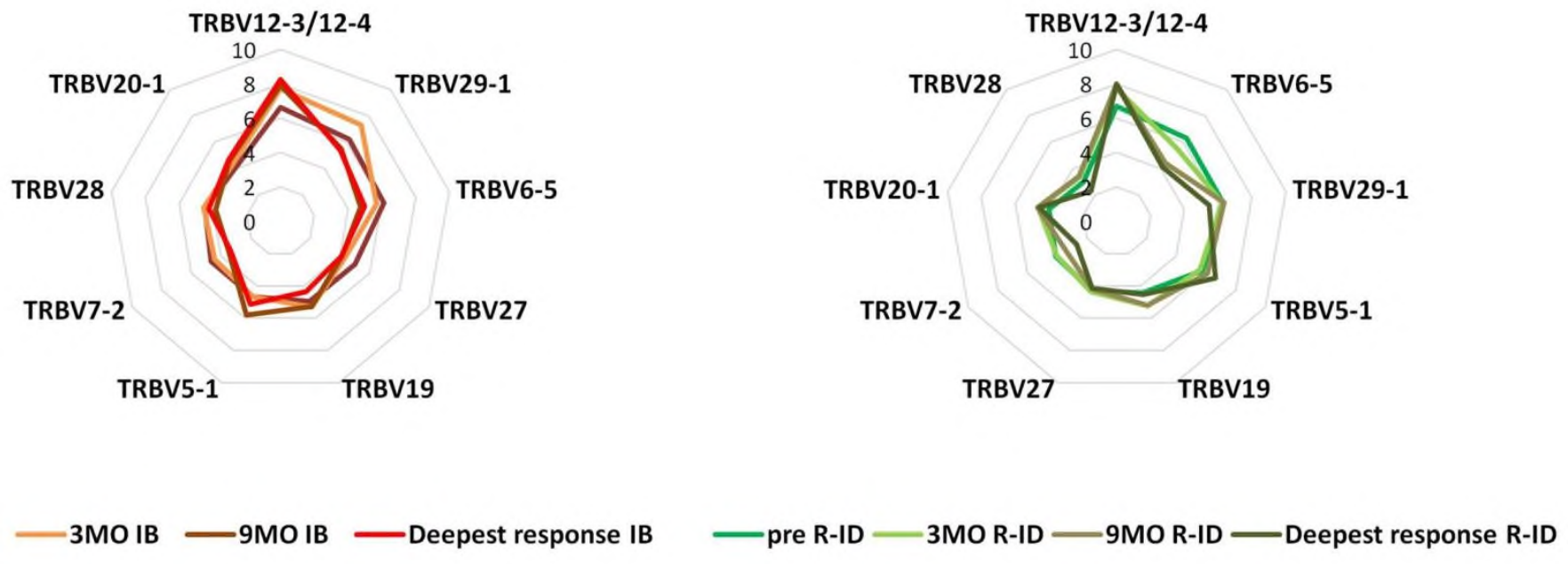


**Suppl. Fig. 2. A. The TRBV gene repertoire remains stable at the 3-month timepoint in all treatment groups.** The % frequency of the 9 most frequent TRBV genes pre-tretament and at the 3-month timepoint per treatment group is depicted. **B. The TRBV gene repertoire remains stable over time for the IB and R-ID groups.** The % frequency of the 9 most frequent TRBV genes pre-treatment, at 3 months, 9 months and deepest clinical response is depicted for the IB and R-ID group.

**Suppl. Fig. 3A**

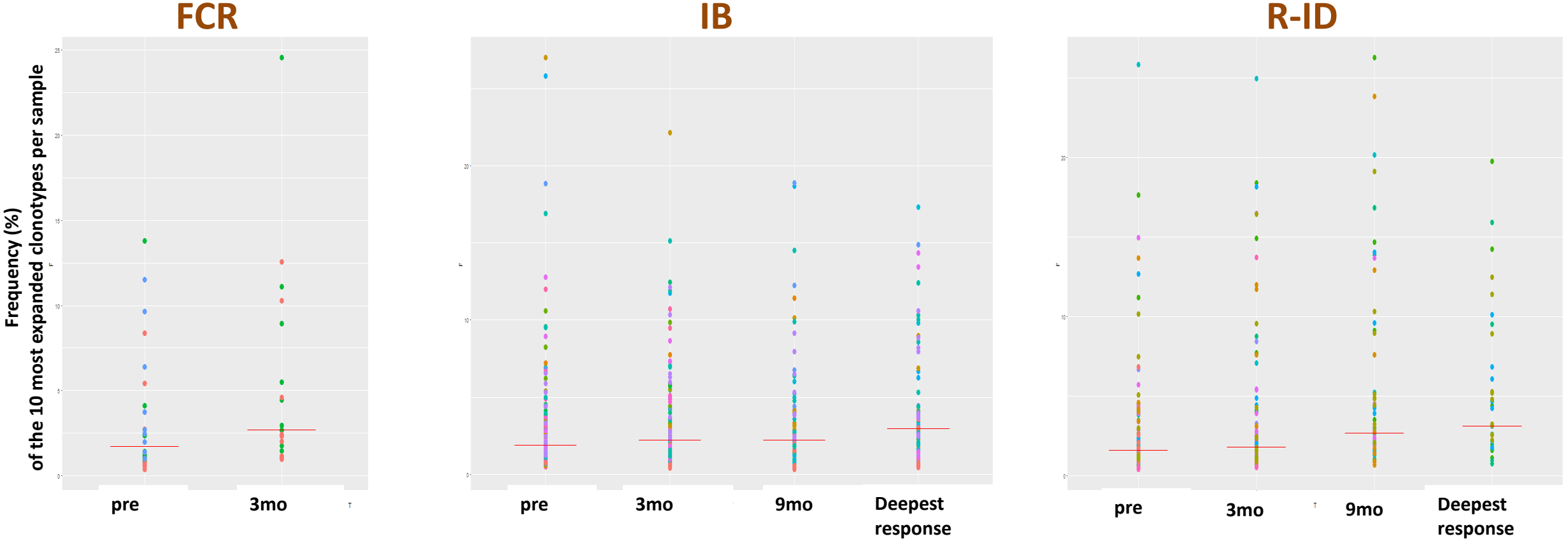
FCR
IB
R-ID
Frequency (%)
of the 10 most expanded clonotypes per sample
pre
3mo
9mo
Deepest response

**Suppl. Fig. 3B**

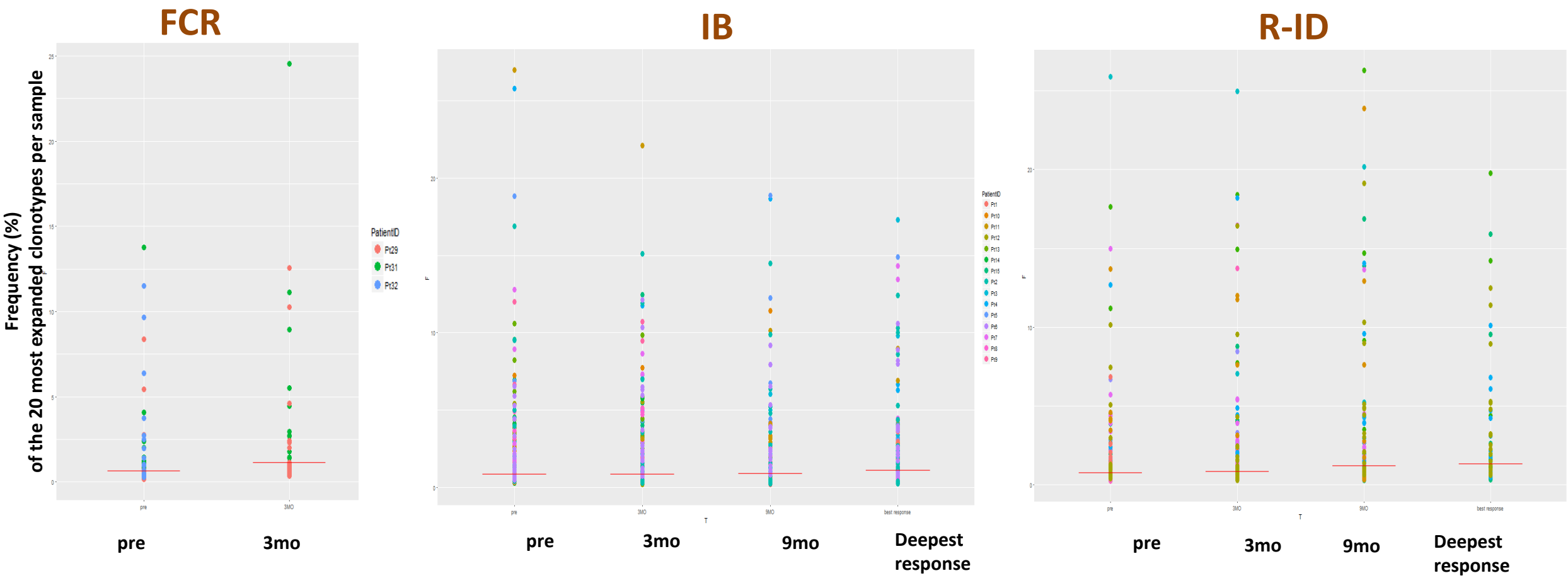
FCR
IB
R-ID
Frequency (%) of the 20 most expanded clonotypes per sample
PatientID
Pt29
Pt31
Pt32
pre
3MO
9MO
best response
T
pre
3mo
pre
3mo
9mo
Deepest response
pre
3mo
9mo
Deepest response

**Suppl. Fig. 3C**

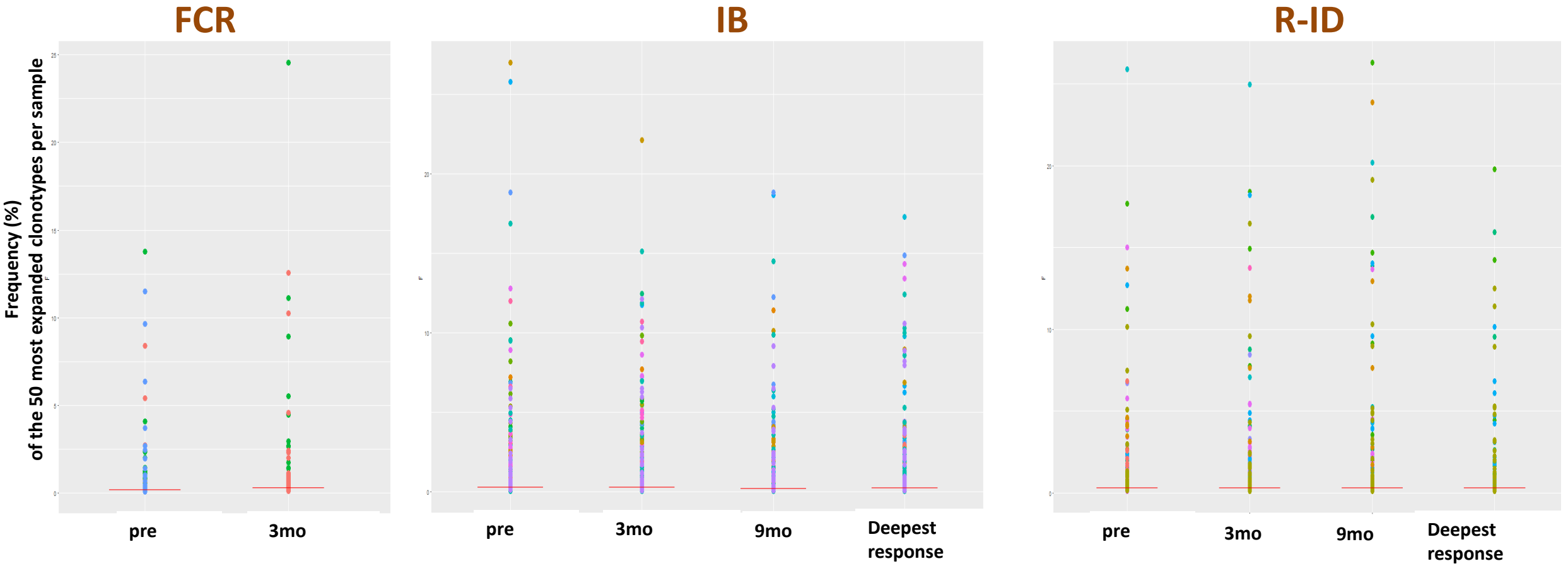
FCR
IB
R-ID
Frequency (%) of the 50 most expanded clonotypes per sample
pre
3mo
pre
3mo
9mo
Deepest response
pre
3mo
9mo
Deepest response

**Suppl. Fig. 3D**

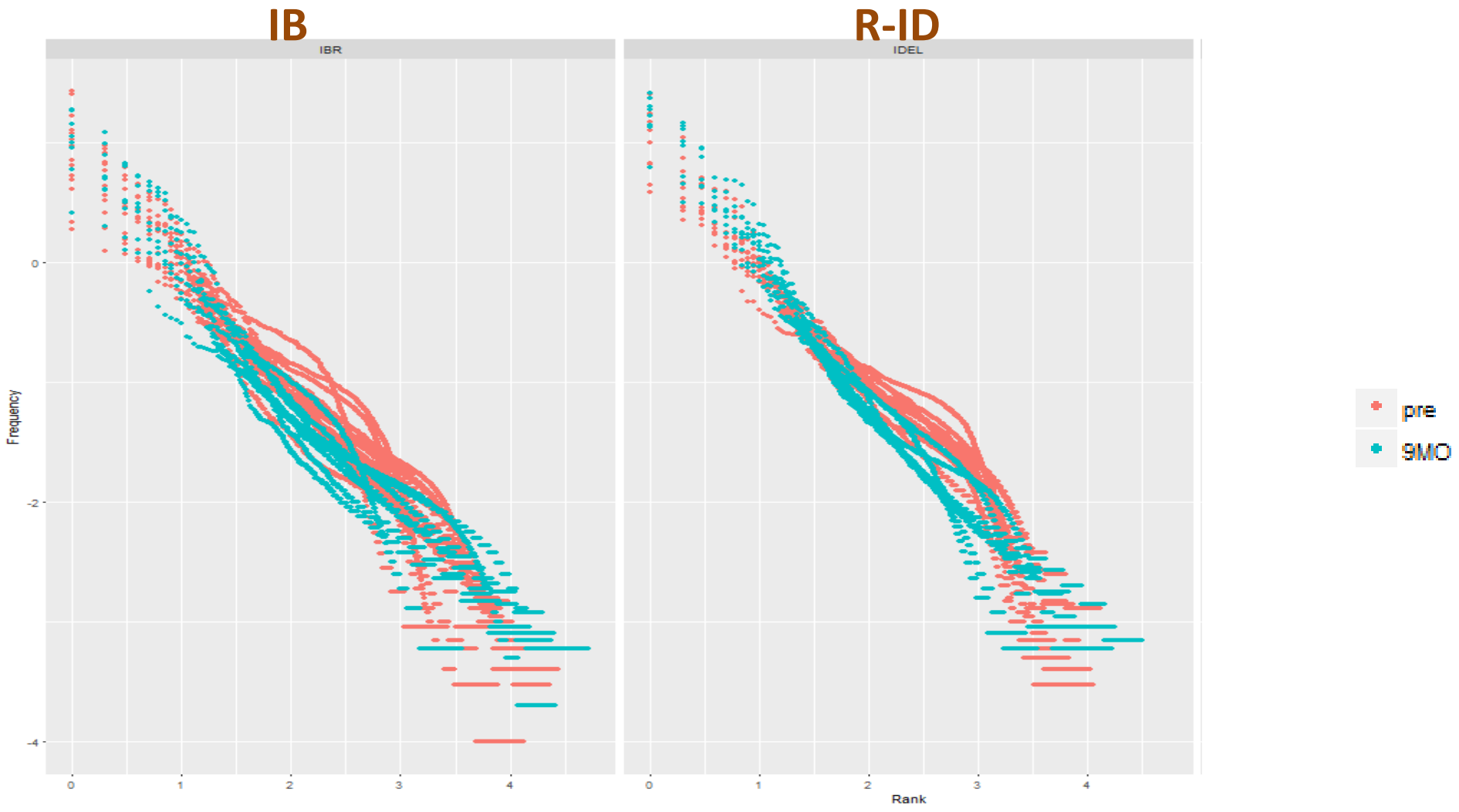


Increase of clonality post-treatment results from the expansion of the major clonotypes. A, B, C: Frequency (%) of the 10, 20 and 50 most expanded clonotypes (dots) per sample overtime, respectively. Clonotypes of the same patient are represented by the same color. The vertical line represents the median value. D: Clonotype frequency against rank plot for the IB and R-ID pre- and +9mo post-treatment.

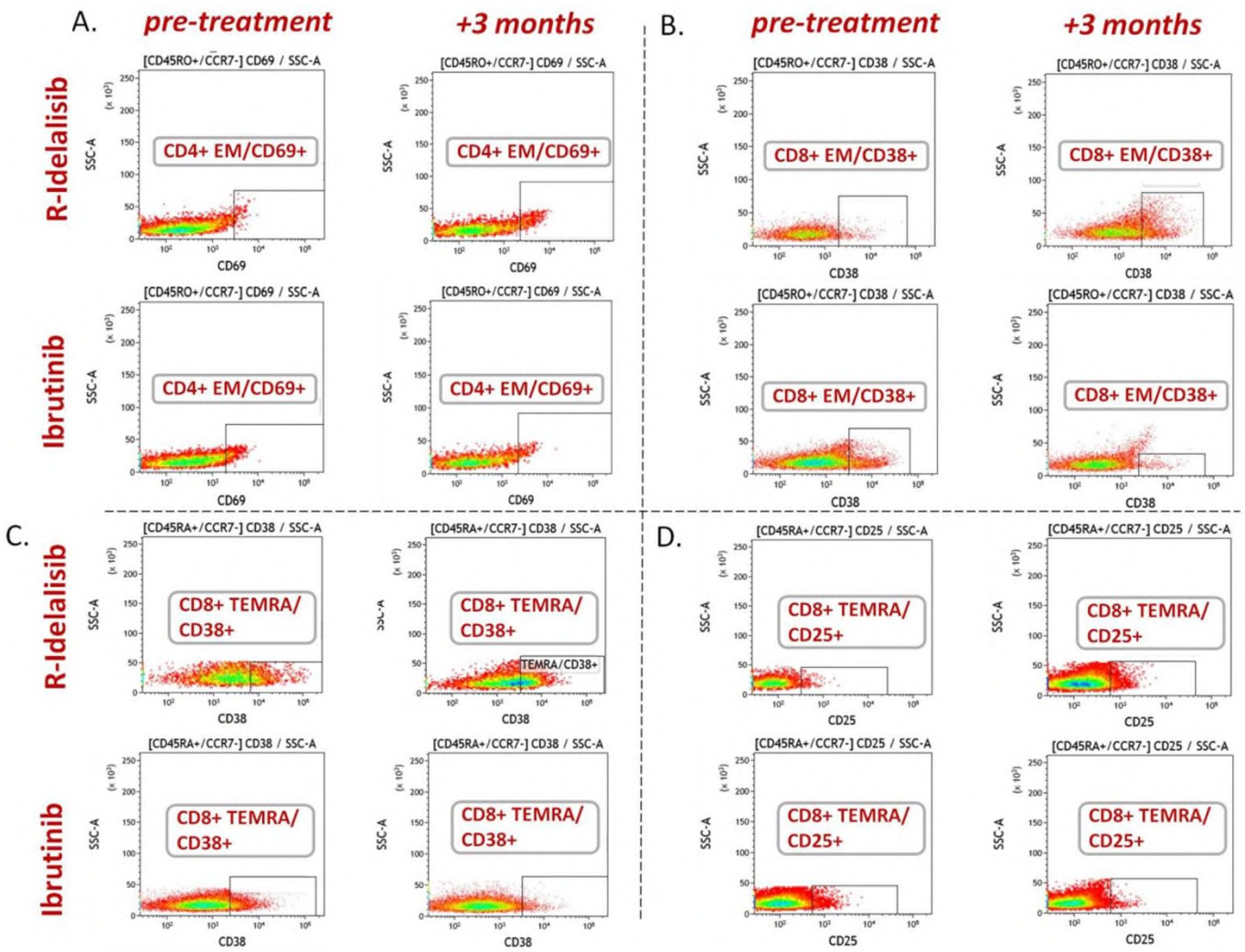


**Suppl. Fig. 4. R-ID increases the expression of activation markers on effector memory T cells as compared to IB treatment.** Each panel (A, B, C, D) shows how treatment affects the expression of an activation marker on a specific T-cell subpopulation for a pair of an R-ID and an IB-treated patient. (A: CD69 expression on $CD4^+$ EM T cells; B: CD38 expression on $CD8^+$ EM T cells; C: CD38 expression on $CD8^+$ TEMRA cells; and, D: CD25 expression on $CD8^+$ TEMRA cells)